RSC Advances

PAPER

View Article Online
View Journal | View Issue

Cite this: *RSC Adv.*, 2019, **9**, 29273

Design, synthesis and biological evaluation of 1,2,3-triazole based 2-aminobenzimidazoles as novel inhibitors of LasR dependent quorum sensing in *Pseudomonas aeruginosa*†

Singireddi Srinivasarao,[a] Adinarayana Nandikolla,[a] Shashidhar Nizalapur,[b] Tsz Tin Yu,[b] Sravani Pulya,[c] Balaram Ghosh,[c] Sankaranarayanan Murugesan,[d] Naresh Kumar[b] and Kondapalli Venkata Gowri Chandra Sekhar*[a]

Bacteria regulate their phenotype, growth and population *via* a signalling pathway known as quorum sensing. In this process, bacteria produce signalling molecules (autoinducers) to recognize their population density. Inhibiting this quorum sensing signalling pathway is one of the potential methods to treat bacterial infection. 2-Aminobenimdazoles are reported to be the strongest inhibitors of quorum sensing against wild-type *P. aeruginosa*. 1,2,3-Triazole based acyl homoserine lactones are found to be good inhibitors of the quorum sensing LasR receptor. Hence, in our current study, forty 1,2,3-triazole based 2-aminobenzimdazoles were synthesized and characterized using IR, NMR, MS and elemental analysis. A single crystal was developed for *N*-(1*H*-benzo[*d*]imidazol-2-yl)-2-(4-nonyl-1*H*-1,2,3-triazol-1-yl)acetamide (**6d**). All final compounds were screened for *in vitro* quorum sensing inhibitory activity against *Pseudomonas aeruginosa*. The quorum sensing inhibitory activity was determined in the LasR expressing *P. aeruginosa* MH602 reporter strain by measuring green fluorescent protein production. Among the title compounds, *N*-(1*H*-benzo[*d*]imidazol-2-yl)-2-(4-(4-chlorophenyl)-1*H*-1,2,3-triazol-1-yl)acetamide (**6i**) exhibited good quorum sensing inhibitory activity of 64.99% at 250 μM. *N*-(1*H*-Benzo[*d*]imidazol-2-yl)-2-(4-(4-nitrophenyl)-1*H*-1,2,3-triazol-1-yl)acetamide (**6p**) exhibited the most promising quorum sensing inhibitory activity with 68.23, 67.10 and 63.67% inhibition at 250, 125 and 62.5 μM, respectively. *N*-(1*H*-Benzo[*d*]imidazol-2-yl)-2-(4-(4-(trifluoromethyl)phenyl)-1*H*-1,2,3-triazol-1-yl)acetamide (**6o**) and *N*-(5,6-dimethyl-1*H*-benzo[*d*]imidazol-2-yl)-2-(4-(4-(trifluoromethyl)phenyl)-1*H*-1,2,3-triazol-1-yl)acetamide (**7l**) also exhibited 64.25% and 65.80% quorum sensing inhibition at 250 μM. Compound **6p**, the most active quorum sensing inhibitor, also displayed low cytotoxicity at the tested concentrations (25, 50 and 100 μM) against normal human embryonic kidney cell lines. Finally, a docking study using Schrodinger Glide elucidated the possible putative binding mode of the significantly active compound **6p** at the active site of the target LasR receptor (PDB ID: 2UV0).

Received 4th July 2019
Accepted 6th September 2019

DOI: 10.1039/c9ra05059k

rsc.li/rsc-advances

1. Introduction

Many pathogenic bacteria use signaling strategies to multiply their number in a process known as Quorum sensing (QS). In this process, bacteria produce and release chemical signaling molecules, known as auto-inducers (AIs). These signaling chemical molecules play a vital role in both bacterial virulence and symbiosis and have a noteworthy impact on human health, cultivation and the environment.[1–3] At high bacterial cell density, bacteria alter gene expression levels to coordinate assorted behaviors, including biofilm formation, virulence factor production, bioluminescence, conjugation, sporulation, *etc.*[4–7] Gram-negative bacteria cause several nosocomial infections including bloodstream infections, pneumonia, wound or surgical site infections.[8,9] *P. aeruginosa*, an opportunistic pathogen and second leading cause of ventilator associated

[a]*Department of Chemistry, Birla Institute of Technology and Science, Pilani, Hyderabad Campus, Jawahar Nagar, Kapra Mandal, Hyderabad – 500078, Telangana, India. E-mail: kvgc@hyderabad.bits-pilani.ac.in; kvgcs.bits@gmail.com; Tel: +91 40 66303527*

[b]*School of Chemistry, UNSW Sydney, NSW 2052, Australia*

[c]*Department of Pharmacy, Birla Institute of Technology and Science, Pilani, Hyderabad Campus, Jawahar Nagar, Kapra Mandal, Hyderabad-500078, Telangana, India*

[d]*Medicinal Chemistry Research Laboratory, Department of Pharmacy, Birla Institute of Technology and Science, Pilani, 333031, India*

† Electronic supplementary information (ESI) available: Experimental procedures for intermediates (chemistry) and spectroscopic/analytical data. CCDC 1904042. For ESI and crystallographic data in CIF or other electronic format see DOI: 10.1039/c9ra05059k

pneumonia is responsible for several serious infections in immune compromised patients, chronic lung infection (cystic fibrosis) and for the most common fatal communicable disease.[10–13] As *P. aeruginosa* develops resistant to available carbapenem and other antibiotics, it is listed as critical by the World Health Organization.[14] Bacterial resistance may cause prolonged hospitalization, expensive medical costs and increase in mortality and hence, there is an urgent need to look out for non-antibiotic solutions to manage invasive bacterial infections and QS could be a potential solution. QSIs are attractive alternatives to replace the conventional antibiotics to minimize the development of bacterial resistance.[15,16] So far, many QSIs have been reported but only very few entered clinical trials.[17] Many proteobacteria which includes *P. aeruginosa* use *N*-acylated-L-homoserine lactones (AHLs/AIs) as QS signaling molecules.[18] (Fig. 1).

P. aeruginosa uses LasI/LasR, RhlI/RhlR and PQS/MvfR QS systems to alter gene expression and is responsible for prolonged hospitalization and high mortality in hospital patients.[19–21] *N*-(3-Oxododecanoyl)-L-homoserine lactone (OdDHL) and *N*-butanoyl-L-homoserine lactone (BHL) are the AIs of *P. aeruginosa* (Fig. 2).[22]

Design

Several AHL and non-AHL based QSIs against *P. aeruginosa* are reported till date.[23,24] Biofilm formation of pathogenic bacteria occurs at high cell-density and higher cell density is responsible for QS.[25–27] Based on this, Blackwell group identified two most active biofilm inhibitors, 2-aminobenzimidazole (**I**) and 5,6-dimethyl-2-aminobenzimidazole (**II**) and evaluated for QSI activity against wild-type *P. aeruginosa* QS reporter strains. Among these, compound **II** possesses higher inhibition against Las and Rhl QS systems with IC_{50} values 37.5 μM and 12.5 μM respectively.[28,29] Furthermore, the same group reported that compound **II** is a potential inhibitor of LasR activity with IC_{50} 2.3 μM against *P. aeruginosa* PAO-JP2 and 1.4 μM against *P. aeruginosa* PAO-JG21 (Fig. 3).[29]

1,2,3-Triazoles are reported as QSIs, antitubercular agents, fluorinated hydrogels and their applications in radiochemistry was also studied previously.[30–35] In 2013, Stacy *et al.* reported AHL based 1,2,3-triazoles as QSIs, in which, they retained the lactone ring of AHL and its amide bond and modified the side chain with various substituted 1,2,3-triazoles and reported effective QSIs against *P. aeruginosa*. Further, they have clearly highlighted that inclusion of triazoles led to superior activity than their counter parts against LasR.[31] Compounds **III** and **IV** are the most active QS inhibitors (Fig. 3), with 75% QS inhibition at 100 μM. In conclusion, this group noticed that compounds with methylene group between *N*-acyl group and 1,2,3-triazole nucleus is indispensable for QSI activity,[31] while compounds with absence of methylene group and *N*-acyl group exhibited poor QSI activity (compounds **V** and **VI**).[32,33] Compounds **VII** and **VIII** are active QSIs with 50.7% and 49.7% inhibition at 250 μM against *P. aeruginosa* MH602 respectively.[34] In another recent work, two methylene linkers retained between triazole nucleus and *N*-acyl-2-phenyl indole gave the most active QSI with 60.8% inhibition at 250 μM against *P. aeruginosa* MH602 (compound **IX**).[24] Compound **X**, with one methylene linker, is an another active QSI with 74.2% inhibition at 250 μM.[35] Based on these results, we retained at least one methylene linker between 1,2,3-triazole and *N*-acyl cycloalkane and designed the compounds of the current scheme (Fig. 3). 1,2,3-Triazole based QSIs are summarized in Table 1.

Enthused by the QSI active molecules of 2-aminonobenzimdazoles and 1,2,3-triazole analogues, we incorporated these active pharmacophores into one framework, and synthesized non-AHL based QSIs, as shown in Fig. 3. In this work, we synthesized various substituted 1,2,3-triazoles of *N*-(1*H*-benzo[*d*]imidazol-2-yl) and *N*-(5,6-dimethyl-1*H*-benzo[*d*]imidazol-2-yl) acetamide, propanamide and butamides and screened them for their QSI activity against *P. aeruginosa* MH602 strain. Several *N*-acyl analogues of cyclopentyl, cyclohexyl and amino pyridines also exhibited promising QSI activity against *P. aeruginosa*.[34] Hence, as a part of this work, we also introduced triazole based *N*-acyl cyclopentane, cyclohexane and pyridine as the tail groups of aminobenzimdazole to gauge their importance in exhibiting QS inhibition.

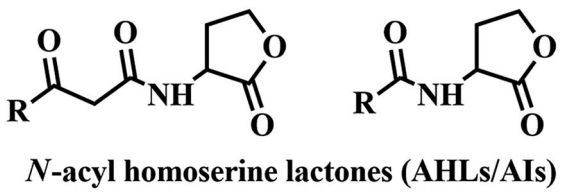

Fig. 1 Autoinducers in proteobacteria.

2. Results and discussion

Chemistry

As shown in Scheme 1, first compounds **2a** and **2b** were prepared according to literature procedure from starting materials **1a** and **1b** respectively.[36] **2a** and **2b** upon treatment with chloroacetyl chloride yielded *N*-acyl compounds **3a** and **3b** respectively. To obtain fourth intermediate, compounds **5a** and **5b** from second **3a** and **3b**, we initially performed several reactions by varying the reaction conditions, which includes the use of different solvents (acetonitrile, tetrahydrofuran, dimethylformamide *etc.*) and temperatures. All these conditions required high temperatures and seal tube/microwave irradiation with long time. Furthermore, KI was used as the catalyst (Finkelstein reaction) and the reaction was carried out in an aprotic solvent in seal tube at 120 °C. It took 72 h for the reaction to proceed but only gave 35% yield. Since satisfactory yields were not obtained even after varying the conditions, we decided to synthesize **5a** and **5b** in two steps. **3a** and **3b** were dissolved in acetone and water to give a clear solution, followed by the addition of 1.2 equivalent of KI and the reaction mixture was heated up to 55 °C for 12 h. On completion of reaction, as indicated by TLC, **4a** and **4b** were isolated. Then pre-final azides **5a** and **5b** were prepared from **4a** and **4b** using NaN_3. Final compounds **6a–q** from **5a** and **7a–n** from **5b** were obtained on treatment with various acetylenes in 45–91% yield (Scheme 1).

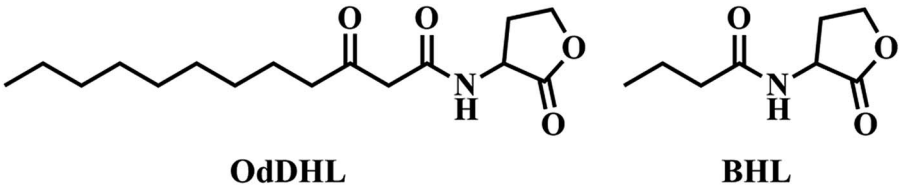

Fig. 2 Auto-inducers in *P. aeruginosa*.

As shown in Scheme 2, in order to get amides **9a–c**, we performed acid-amine coupling reaction using EDC·HCl and HOBt as coupling reagents. Compound **9a** was prepared from 1*H*-benzo[*d*]imidazol-2-amine (**2a**) and pent-4-ynoic acid (**8a**). Similarly, **2a** and **2b** on treatment with hex-5-ynoic acid (**8b**) yielded compounds **9b** and **9c** respectively. Finally, the **9a**, **9b** and **9c** on treatment with various substituted azides using copper sulphate pentahydrate as catalyst gave **10a–b**, **11a–d** and **12a–c** in 45–68% yield.

Most of the azides required for triazole preparation were procured commercially. However, azides **A**, **B** and **C** required for the preparation of the final derivatives of **Series-III** were accomplished *via* Scheme 3.

The purity of the synthesized compounds was assessed by LC-MS and elemental analyses. Structures of the compounds were confirmed by spectral data. In ^{1}H NMR and ^{13}C NMR, the signals of the corresponding protons and carbon atoms were verified based on their chemical shift, multiplicities and coupling constant values. The results of elemental analysis were within ±0.05 of the theoretical values.

^{1}H NMR spectra of compounds **6a–q** and **7a–n** from Scheme 1 showed singlet which integrates to two protons at 5–6 ppm due to the active methylene CH_2, whereas the methylene protons for compounds **10–12** from Scheme 2 were observed at more up field (at around 1.5 to 3.5 ppm) due to a larger separation of methylene protons from *N*-acyl group and triazole nucleus. All final compounds from Schemes 1 and 2 have

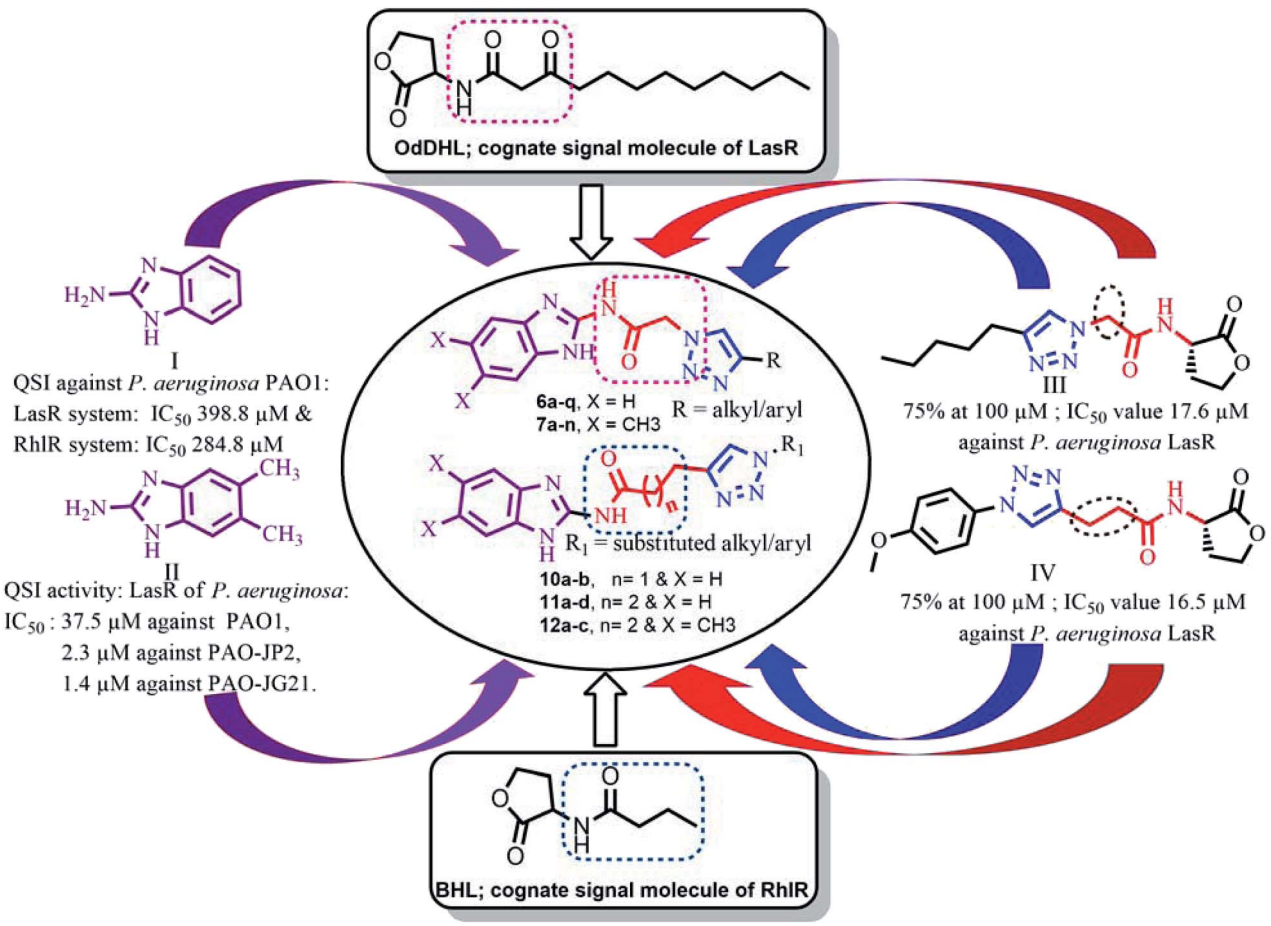

Fig. 3 Design strategy for the synthesis of titled quorum sensing inhibitors.

Table 1 1,2,3-Triazole based QSIs against *P. aeruginosa* reported from literature

Entry	Compound number	Structures of QSIs	% Inhibition against *P. aeruginosa*	Reference no.
1	**III**	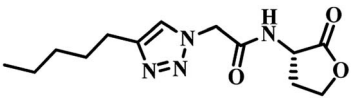	75% at 100 μM	31
2	**IV**	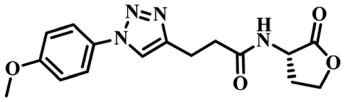	75% at 100 μM	31
3	**V**	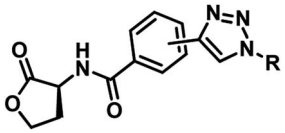	Ranged from 0 to 49.9% at 1 mM concentration	32
4	**VI**	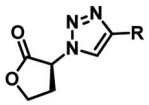	Ranged from 1 to 22% at 100 μM	33
5	**VII** & **VIII**	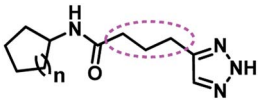	$n = 1$; **VI** 50.7% at 250 μM $n = 2$; **VII** 49.7% at 250 μM	34 34
6	**IX**	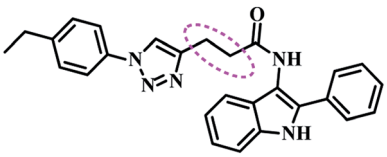	60.8% at 250 μM	24
7	**X**	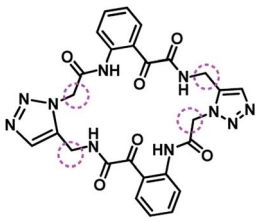	74.2% at 250 μM	35

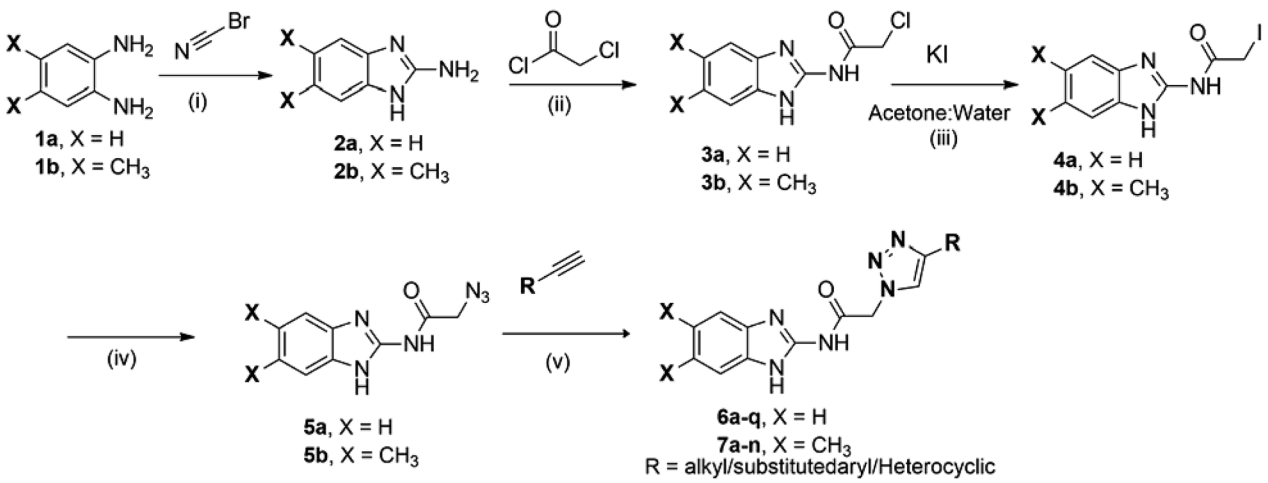

Scheme 1 General synthetic route for compounds **6a–q** and **7a–n**. Reagents and conditions: (i) cyanogen bromide (1.1 eq.), methanol, reflux, 5 min; (ii) chloroacetyl chloride (1.0 eq.), pyridine (2.5 eq.), CH_2Cl_2, 0 °C-rt, 12 h; (iii) potassium iodide (1.2 eq.), acetone, 55 °C, 12 h; (iv) NaN_3 (1.5 eq.), DMF : water (8 : 2), 0 °C; (v) substituted terminal alkynes (1.4 eq.), $CuSO_4 \cdot 5H_2O$, (5 mol%), sodium ascorbate (10 mol%), DMF : water (8 : 2), rt, 6–16 h.

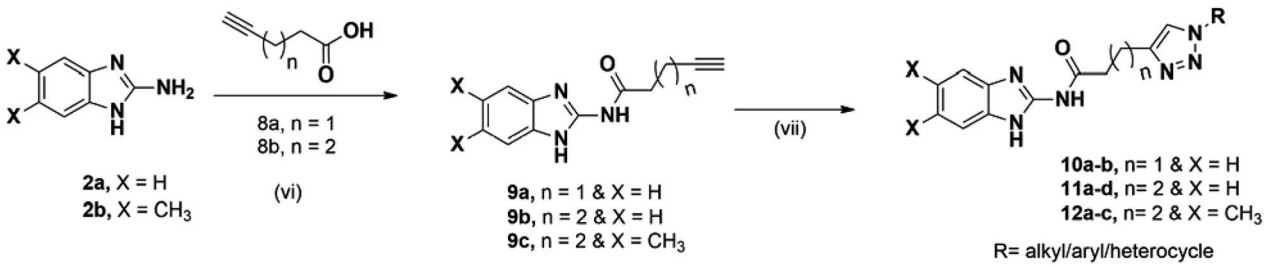

Scheme 2 General synthetic route for compounds **10a–b**, **11a–d** and **12a–c**. Reagents and conditions: (vi) **2a** or **2b** (1.0 eq.), EDC·HCl (1.5 eq.) HOBt, (1.5 eq.) diisopropyl ethylamine (2.5 eq.), DMF, rt, 16 h; (vii) **9a**/**9b**/**9c** and substituted azides (1.5 eq.), $CuSO_4 \cdot 5H_2O$, (10 mol%), sodium ascorbate (10 mol%), DMF : water (8 : 2), rt, 6–16 h.

triazole nucleus, benzimidazole N–H and amide N–H, in which the proton of triazole nucleus was observed at around 8.2–9.2 ppm as singlet, and the N–H protons of amide and imidazole were observed as broad singlets at 11–14 ppm. Furthermore, single crystal was developed for compound **6d**.

Biological activity

Series of triazole based benzimidazole derivatives (**6a–q**, **7a–n**, **10a–b**, **11a–d** and **12a–c**) were analyzed for their QS-inhibition activity at various concentrations (62.5, 125 & 250 μM) against *P. aeruginosa* MH602 lasB reporter strain [PlasB: gfp(ASV)] following the protocol developed by Hentzer *et al.*[37] The production of AHL signals by this reporter strain leads to an increase in the production of unstable green fluorescent protein (GFP-ASV) as a function of an active QS system. Considering this fact, synthesis of benzimidazole triazole analogues has been prioritized to counteract the QS system. The results are compiled in Table 2.

Predictive structure–activity relationship study (SAR)

In the first series (**Series-I** in Table 2), benzimidazoles **6a–q** with no substitution on the benzene ring were undertaken. The effect of alkyl chain length on the triazole partner of the molecule was first studied. It was found that changing the lipophilicity by altering the length of the alkyl chain on triazole ring has no significant effect on the QSI activities of the compound as compounds **6a–d** possess similar percentage of QS inhibition within different tested concentrations. The effect of attaching a terminal heterocyclic group on the triazole partner of the molecule was then studied. While attaching a 2-methylthiobenzimidazole onto the triazole ring (**6e**) gave a similar QSI activity (41.31% inhibition at 250 μM) as compounds **6a–d** (42.76–50.50% inhibition at 250 μM), it was found that attaching 5-chloro-pyridone on the triazole nucleus (**6f**) enhanced the QSI activity of benzimidazole to 58.84% at 250 μM. The QSI activities of benzimidazoles having various substituted aryl groups on triazole nucleus (**6g–q**) were also investigated. Halo-substitution at the *para*-position of aryls on the triazole nucleus (**6h–j**) showed promising QSI activity even at low concentration (>45.00% inhibition at 62.5 μM) when compared to its un-substituted parent molecule **6g**, with only 15.10% inhibition at 62.5 μM. Furthermore, among these halo-aryl derivatives, chloro-derivative (**6i**) exhibited the highest QSI activity at all concentrations. Alkyl groups substituted at the *para*-position of aryl ring (**6k–l**) diminished the QSI activity of the benzimidazoles. In fact, when a *tert*-butyl group was placed on the aryl ring of the triazole nucleus, the corresponding benzimidazole (**6l**) showed no QSI activity at lower concentrations. To study the effect of aryl rings carrying electron-releasing groups on the QSI activity, benzimidazoles **6m** and **6n** bearing a phenol and anisole group, respectively, were tested.

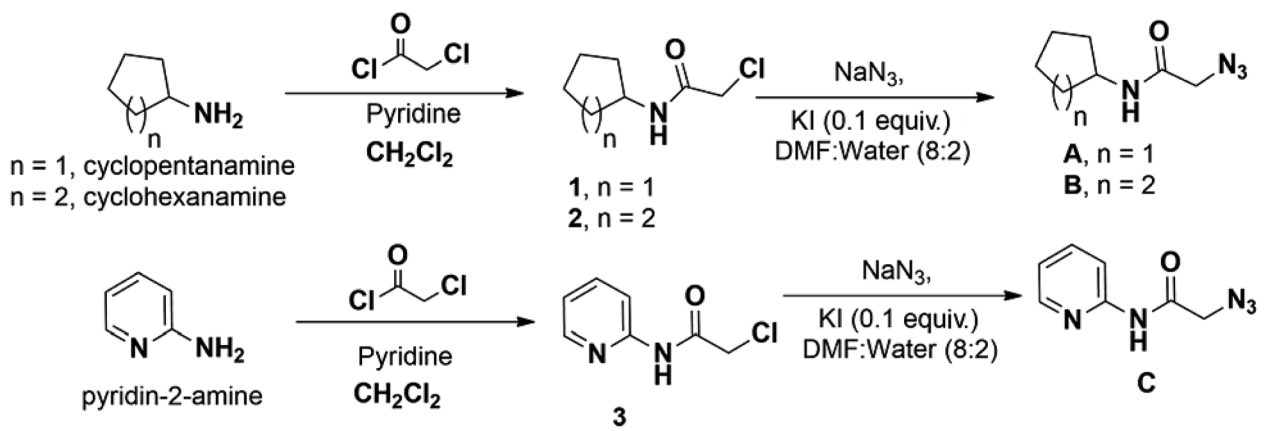

Scheme 3 General synthetic route for intermediates A, B and C.

Table 2 Percentage inhibition of GFP fluorescence by the synthesized compounds against *P. aeruginosa* MH602

Entry	R	R_1	X	*n*	Concentration[a] (μM) 250	125	62.5
Series-I							
6a		—	H	—	50.50 ± 11.81	35.28 ± 20.43	25.10 ± 0.37
6b		—	H	—	43.47 ± 6.23	38.77 ± 11.47	27.37 ± 2.36
6c		—	H	—	42.76 ± 14.58	34.69 ± 11.60	25.68 ± 7.62
6d		—	H	—	48.55 ± 12.66	41.93 ± 4.50	30.61 ± 7.62
6e	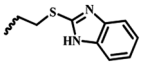	—	H	—	41.31 ± 7.90	37.20 ± 6.71	24.87 ± 6.69
6f	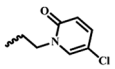	—	H	—	58.84 ± 5.09	52.70 ± 11.86	36.07 ± 10.70
6g		—	H	—	45.95 ± 10.15	17.43 ± 21.96	15.10 ± 5.83
6h	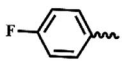	—	H	—	56.14 ± 1.77	54.85 ± 2.42	48.95 ± 12.32
6i	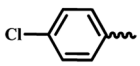	—	H	—	**64.99 ± 8.25**	**60.55 ± 6.16**	**52.86 ± 8.86**
6j	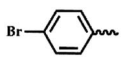		H	—	50.74 ± 10.91	46.25 ± 8.52	45.68 ± 5.44
6k	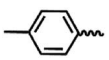	—	H	—	35.85 ± 13.83	32.32 ± 22.23	36.82 ± 6.63
6l	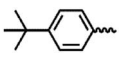	—	H	—	35.22 ± 8.78	NA	NA
6m	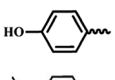	—	H	—	58.44 ± 7.75	45.66 ± 6.21	34.37 ± 4.97
6n	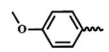	—	H	—	20.03 ± 14.00	5.16 ± 16.63	NA
6o	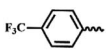	—	**H**	—	**64.25 ± 7.30**	**59.85 ± 7.99**	**57.55 ± 7.73**
6p	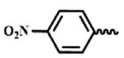	—	H	—	**68.23 ± 3.87**	**67.10 ± 5.45**	**63.67 ± 7.51**
6q		—	H	—	39.37 ± 5.14	36.04 ± 6.13	28.21 ± 10.23
Series-II							
7a		—	CH_3	—	31.76 ± 10.99	22.05 ± 14.66	19.85 ± 3.80
7b		—	CH_3	—	26.59 ± 20.80	20.22 ± 11.52	16.92 ± 5.74
7c		—	CH_3	—	NA	NA	NA
7d		—	CH_3	—	44.57 ± 3.87	41.65 ± 5.08	37.11 ± 7.75
7e	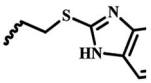	—	CH_3	—	16.00 ± 26.10	NA	15.13 ± 9.82
7f	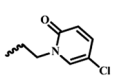		CH_3	—	36.80 ± 7.90	29.03 ± 13.57	26.08 ± 7.69

Table 2 (*Contd.*)

Entry	R	R_1	X	*n*	Concentration[a] (μM) 250	125	62.5
7g		—	CH_3	—	47.56 ± 14.43	29.85 ± 17.40	28.51 ± 8.41
7h	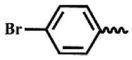	—	CH_3	—	57.60 ± 7.43	44.67 ± 14.27	31.23 ± 5.02
7i	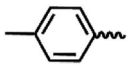	—	CH_3	—	50.74 ± 12.31	14.91 ± 8.82	NA
7j	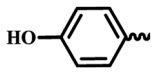	—	CH_3	—	44.73 ± 13.15	24.16 ± 14.52	17.62 ± 6.21
7k	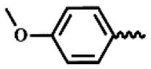	—	CH_3	—	40.82 ± 23.41	24.30 ± 23.26	20.38 ± 2.59
7l	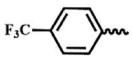	—	CH_3	—	**65.80 ± 1.91**	**56.44 ± 5.85**	**36.13 ± 7.67**
7m	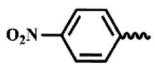	—	CH_3	—	53.85 ± 9.78	31.46 ± 16.18	21.02 ± 10.29
7n	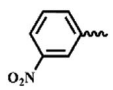	—	CH_3	—	46.73 ± 4.87	34.42 ± 14.10	34.20 ± 7.43
Series-III							
10a	—	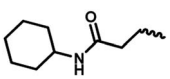	H	1	47.40 ± 2.69	42.35 ± 8.46	38.43 ± 7.72
10b	—	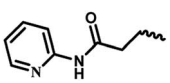	H	1	28.46 ± 17.54	15.64 ± 7.17	4.40 ± 2.93
11a	—	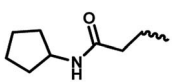	H	2	51.23 ± 7.10	45.93 ± 8.18	42.27 ± 10.29
11b	—	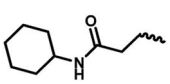	H	2	12.87 ± 20.18	NA	NA
11c	—	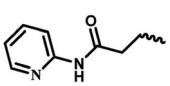	H	2	19.41 ± 8.16	15.69 ± 8.81	3.69 ± 11.15
11d	—	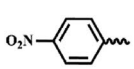	H	2	39.38 ± 4.60	21.37 ± 2.62	21.17 ± 1.76
12a	—	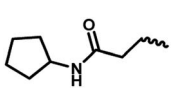	CH_3	2	48.48 ± 5.25	34.14 ± 12.60	28.54 ± 7.69
12b	—	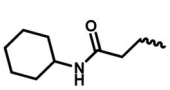	CH_3	2	30.83 ± 26.38	9.74 ± 20.67	5.35 ± 10.20
12c	—	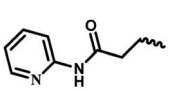	CH_3	2	48.26 ± 13.42	7.07 ± 11.80	NA
Furanone 30	—	—		—	86.86 ± 1.18	83.02 ± 3.15	77.33 ± 2.00

[a] Growth inhibition, ±standard deviation of the mean from at least two independent experiments. In each independent experiment, compounds were tested in triplicate. NA: no activity.

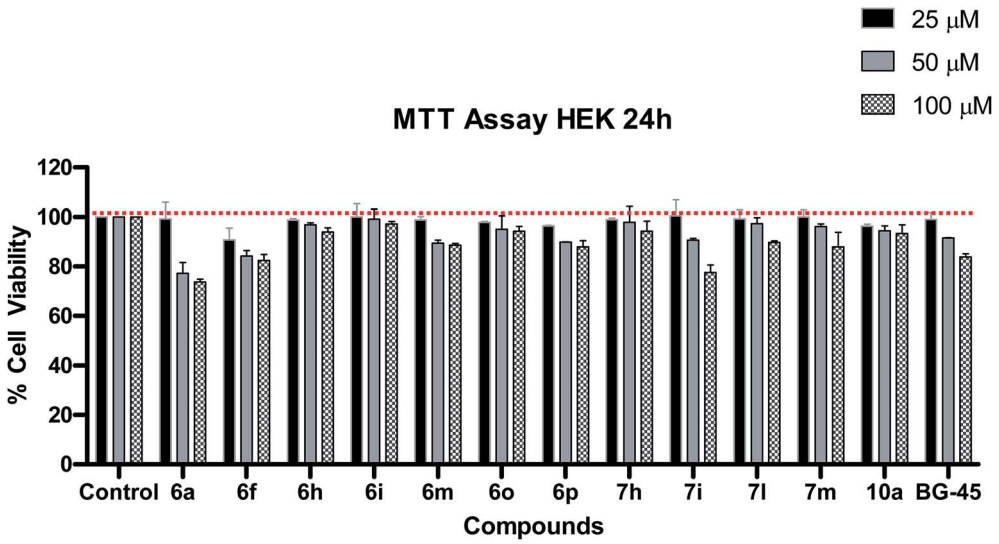

Fig. 4 Cytotoxicity study of the most active QSIs in HEK-293 cells by MTT assay after 24 h compound treatment. BG45 was used as a positive control. Data represents mean ± SD ($n = 3$).

Benzimidazoles **6m** with a phenol group present on the triazole nucleus possesses moderate QSI activity at low concentrations (34.37% at 62.5 μM), however, when the phenol group was substituted by a different electron-releasing anisole group (**6n**), the QSI activity of the molecule was completely abolished. This suggested that QSI activity of a compound could not be correlated by attaching an electron-releasing group at the *para*-position of the phenyl ring on the triazole nucleus. Following this finding, the effect of substituting electron withdrawing groups on the aryl ring towards QS inhibition was studied. Benzimidazole compound **6o** bearing a trifluoromethyl group on the aryl ring exhibited a significantly higher QSI activity (57.55% inhibition at 62.5 μM) when compared to its parent compound **6g** (with only 15.10% inhibition at 62.5 μM) and the QSI activity is further enhanced by substituting more electron-withdrawing nitro group at *para*-position of the phenyl ring, with compound **6p** showed 63.67% inhibition at 62.5 μM. However, when the nitro group was moved to the *meta*-position (**6q**), QSI activity was diminished (28.21% at 62.5 μM). From the QSI data of this series, it can be concluded that, QSI activity of the benzimidazole molecule is favored by the presence of aryl ring with a *para*-substituted electron-withdrawing group on the triazole nucleus.

In the second part of the series (**Series-II**), benzimidazoles **7a–n** bearing di-methyl substitution on the benzene ring was considered as basic moiety and the effect of substitution on the triazole nucleus towards the QSI activity was investigated. When alkyl groups of different lengths were placed on the triazole nucleus, dimethylbenzimidazole (compound **7d**) with the longest carbon chain exhibited moderate activity (44.57% at 250 μM). The QSI activity of the compounds reduced while decreasing the alkyl chain length. When introducing heterocyclic groups such as 2-methylthio-benzimidazole (**7e**) and 5-chloro-pyridone (**7f**) onto the triazole nucleus, the analogues only showed mild inhibitory activity even at the highest tested concentration. In another attempt, various aryl groups bearing different substituents on triazole nucleus were investigated. The presence of an electron-donating methyl group at the 4-position of the aryl ring (**7i**) did not impact the inhibitory activity at higher doses (50.74% at 250 μM) when compared to its un-substituted parent molecule **7g**, in fact, it hampered the QSI inhibition at lower concentrations. The presence of other electron-donating groups such as hydroxyl (**7j**) and alkoxy (**7k**) at the 4-position of the phenyl ring were also found to be effective only at higher concentrations (>40% at 250 μM). In case of aryl rings possessing electron withdrawing groups, trifluoromethyl group at *para*-position enhanced the QSI activity of the dimethylbenzimidazole (65.80% at 250 μM), while other nitro substituted aryl partners were effective only at higher concentrations (**7m** & **7n**). It can be concluded that aryl substituted triazole nucleus based dimethylbenzimidazole derivatives displayed better QS inhibition activity when electron withdrawing groups are present on the aryl ring.

Apart from the above moieties studied so far, few more 2-aminobenzimidazole derivatives were designed and synthesized by altering the length of carbon chain between the amido functional group and the triazole moiety as well as placing different functionalities on triazole nucleus (**Series-III**). All these moieties were explored for their QSI at reported concentrations. In the first part of this series, the chain length between the 2-amido benzimidazole and the triazole nucleus was fixed at two and two analogues **10a** and **10b** were synthesized by retaining different substitutions on the triazole nucleus. Among these, *N*-cyclohexyl acetamido substitution at the triazole (**10a**) showed good QSI activity regardless of the concentration (38–47% at 62.5–250 μM). In the later series, the length of the carbon chain between the 2-amido benzimidazole and the triazole nucleus was increased to three. Four benzimidazoles (**11a–d**) with the three carbon chain length were synthesized and tested for their QSI activity. It was found that triazole carrying *N*-cyclopentyl

Table 3 *In silico* predicted physico-chemical and pharmacokinetic parameters of the titled compounds

Entry	Mol. wt[a]	SASA[b]	HBD[c]	HBA[d]	log Po/w[e]	PCaco[f]	log BB[g]	log S[h]	Rot. bonds[i]
6a	284.32	567.436	0	3.5	3.038	343.769	−1.286	−4.161	6
6b	312.374	636.971	0	3.5	3.92	429.085	−1.412	−5.153	8
6c	340.427	711.635	0	3.5	4.822	498.442	−1.569	−6.242	10
6d	368.481	743.435	0	3.5	5.268	305.705	−1.907	−6.519	12
6e	404.448	584.577	1	5.0	3.838	605.209	−0.839	−4.174	7
6f	383.796	530.836	0	6.5	2.171	267.446	−0.934	−2.154	6
6g	318.337	564.382	0	3.5	3.461	357.559	−1.068	−4.428	4
6h	336.328	567.032	0	3.5	3.647	353.871	−0.952	−4.683	4
6i	352.782	586.704	0	3.5	3.94	351.095	−0.933	−5.163	4
6j	397.233	589.559	0	3.5	4.025	354.108	−0.911	−5.242	4
6k	332.364	594.968	0	3.5	3.794	375.045	−1.088	−5.008	4
6l	374.444	636.388	0	3.5	4.559	358.01	−1.138	−5.63	5
6m	334.337	570.734	1	4.25	2.794	106.664	−1.634	−4.336	5
6n	348.363	629.418	0	4.25	3.834	519.109	−1.094	−5.105	5
6o	386.336	598.845	0	3.5	4.344	358.282	−0.799	−5.59	4
6p	363.335	610.671	0	4.5	2.762	42.587	−2.146	−4.619	5
6q	363.335	630.124	0	4.5	3.014	61.546	−2.088	−4.988	5
7a	312.374	631.212	0	3.5	3.818	475.547	−1.228	−5.369	6
7b	340.427	671.361	0	3.5	4.387	413.083	−1.414	−5.715	8
7c	368.481	753.598	0	3.5	5.352	506.822	−1.573	−7.037	10
7d	396.534	826.137	0	3.5	6.173	496.042	−1.803	−8.086	12
7e	432.502	774.439	1	5.0	4.777	146.42	−1.994	−7.549	7
7f	411.85	546.498	0	6.5	2.611	358.622	−0.82	−2.398	6
7g	346.391	593.336	0	3.5	3.9	361.81	−1.048	−4.977	4
7h	425.287	623.302	0	3.5	4.458	341.091	−0.935	−5.879	4
7i	360.418	620.804	0	3.5	4.176	339.567	−1.108	−5.498	4
7j	362.39	591.857	1	4.25	3.165	104.014	−1.59	−4.71	5
7k	376.417	617.631	0	4.25	4.029	420.983	−1.026	−4.882	5
7l	414.389	700.508	0	3.5	5.396	514.904	−0.833	−7.521	4
7m	391.388	639.666	0	4.5	3.217	43.007	−2.11	−5.169	5
7n	391.388	559.1	0	4.5	2.89	93.403	−1.454	−3.642	5
10a	395.463	752.156	2	8.0	2.322	85.992	−2.006	−4.778	7
10b	390.404	576.151	2	9.0	1.653	229.916	−1.278	−2.688	7
11a	395.463	765.567	2	8.0	2.482	90.546	−2.062	−4.838	8
11b	409.49	800.267	2	8.0	2.778	87.077	−2.169	−5.447	8
11c	404.43	778.651	2	9.0	2.694	104.37	−2.408	−5.789	8
11d	391.388	720.921	1	6.0	3.206	49.823	−2.531	−6.191	6
12a	423.517	841.741	2	8.0	3.099	110.476	−2.224	−6.492	8
12b	437.544	842.109	2	8.0	3.317	87.762	−2.177	−6.169	8
12c	432.484	835.341	2	9.0	3.272	107.993	−2.472	−6.752	8

[a] Mol. wt – molecular weight (130–725). [b] SASA – solvent accessible surface area (300–1000). [c] HBD – no. of hydrogen bond donors (0–6). [d] HBA – no. of hydrogen bond acceptors (2 to 20). [e] log Po/w – predicted octanol/water partition coefficient (−2.0–6.5). [f] Caco – 2 cell permeability in nm s^{-1} (<25 poor, >500 great). [g] log BB – predicted brain/blood partition coefficient (−3.0–1.2). [h] log S – aqueous solubility of a compound (−6.5–0.5 mol dm^{-3}). [i] Rot – no. of rotatable bonds (0 to 15).

acetamido group (**11a**) was identified to be the most potent compound in this series and its potency was retained even at lower concentration (42.27% at 62.5 μM). On the other end, compound **11d** with 4-nitrophenyl group on triazole nucleus was active only at high doses (39.38% at 250 μM). The remaining analogues **11b–c** were less potent even at highest tested concentration. Finally, by maintaining three carbon chain length, various dimethylbenzimidazoles were also investigated. Dimethylbenzimidazoles possessing *N*-(2-pyridyl)-acetamido group on triazole nucleus (**12c**) showed moderate inhibition activity only at high concentration (48.26% at 250 μM) and its inhibition activity was diminished when its concentration was halved. The same trend was observed for compound **12b** with a *N*-cyclohexyl acetamido group placed at the triazole nucleus. On the other hand, compound **12a** exhibited moderate inhibition activity at 250 μM. While its inhibition activity reduces with the decrease in concentration, the magnitude of the reduction was smaller than that of compounds **12b–c**. It can be concluded that *N*-(2-pyridyl), *N*-cyclopentyl and *N*-cyclohexyl acetamido substituted triazoles exhibited moderate QSI activity at high concentration within this series.

Overall, it can be concluded that, most of the scaffolds in this study possess moderate to high inhibition activity at high concentration and compounds **6i**, **6o**, **6p** and **7l** exhibited significant QSI activity at all the reported concentrations and were

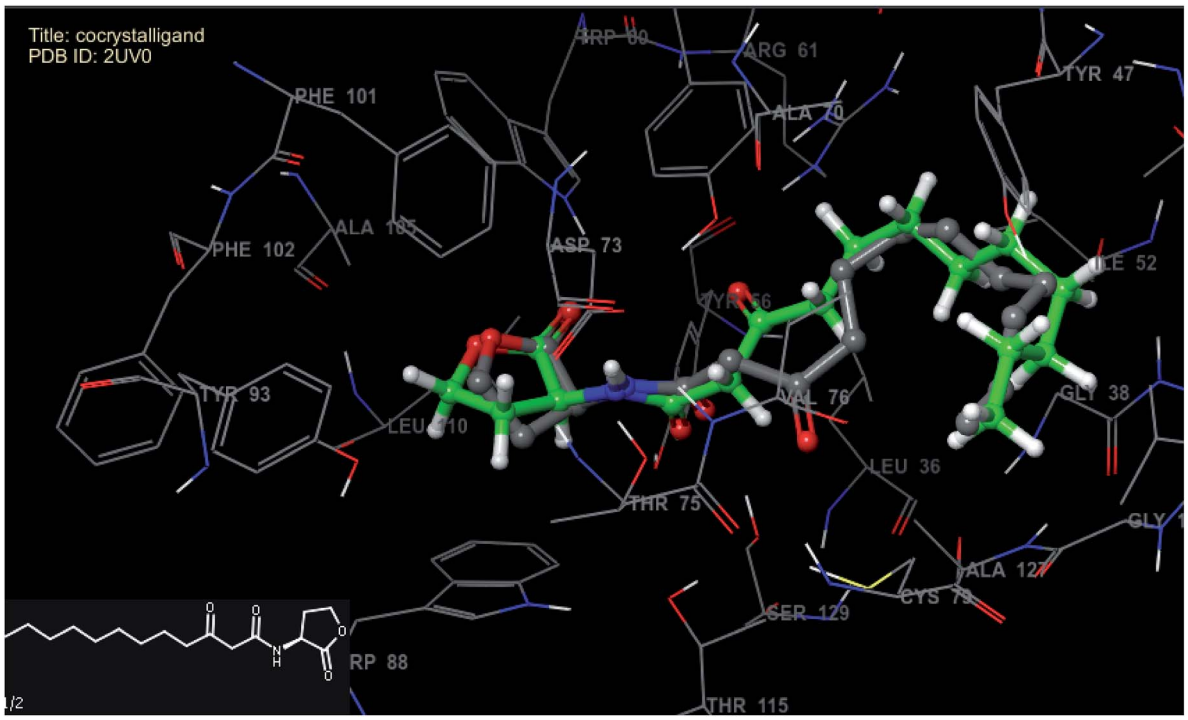

Fig. 5 Superimposed view of best scoring native pose of co-crystallized (grey) ligand with its X-ray pose (green) inside the active site of 2UV0.

identified to be the most active compounds in this study. Most of the compounds reported in the current work exhibited comparable activity to the previously reported triazoles as shown in Table 2. The most active compound from this study, **6p** is better than the previously reported compounds (**V–IX** of Table 1).

Cytotoxicity studies

On the basis of QS inhibitory activity, the significantly active compounds (**6a**, **6f**, **6h**, **6i**, **6m**, **6o**, **6p**, **7h**, **7i**, **7l**, **7m** and **10a**) were evaluated for their cytotoxicity against Human Embryonic Kidney cell lines (HEK-293) at 25, 50 and 100 μM

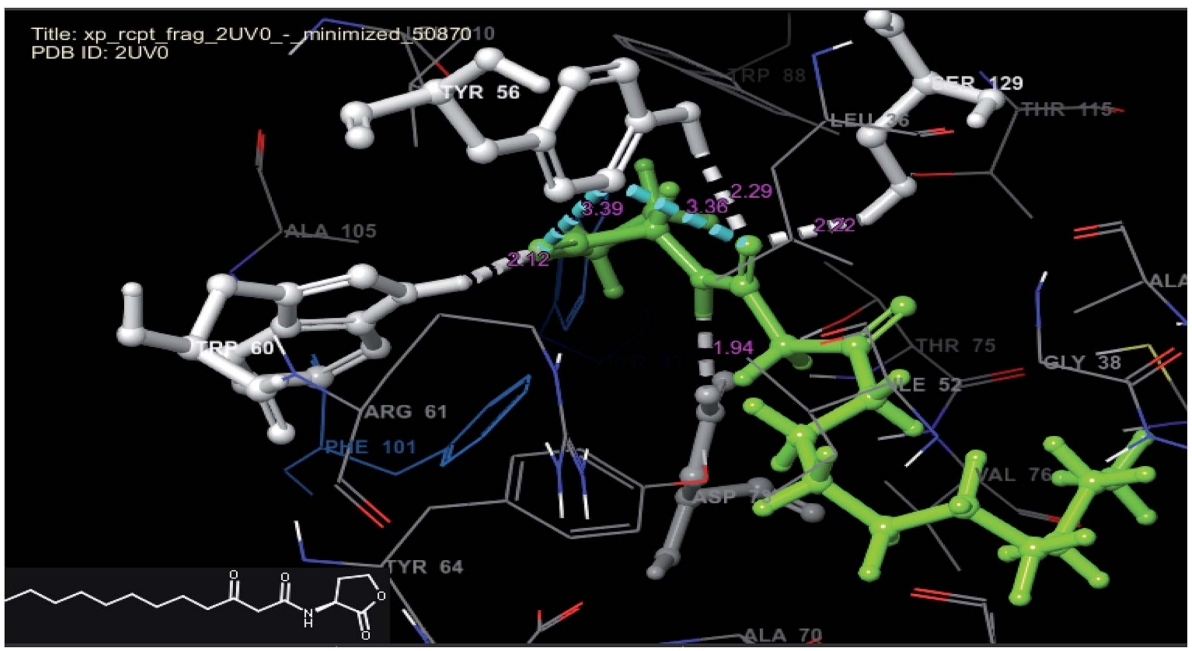

Fig. 6 Docked pose view of co-crystallized ligand with interactions and distances (color interpretation: white-hydrogen bond, blue pi–pi stacking) inside the active site of 2UV0.

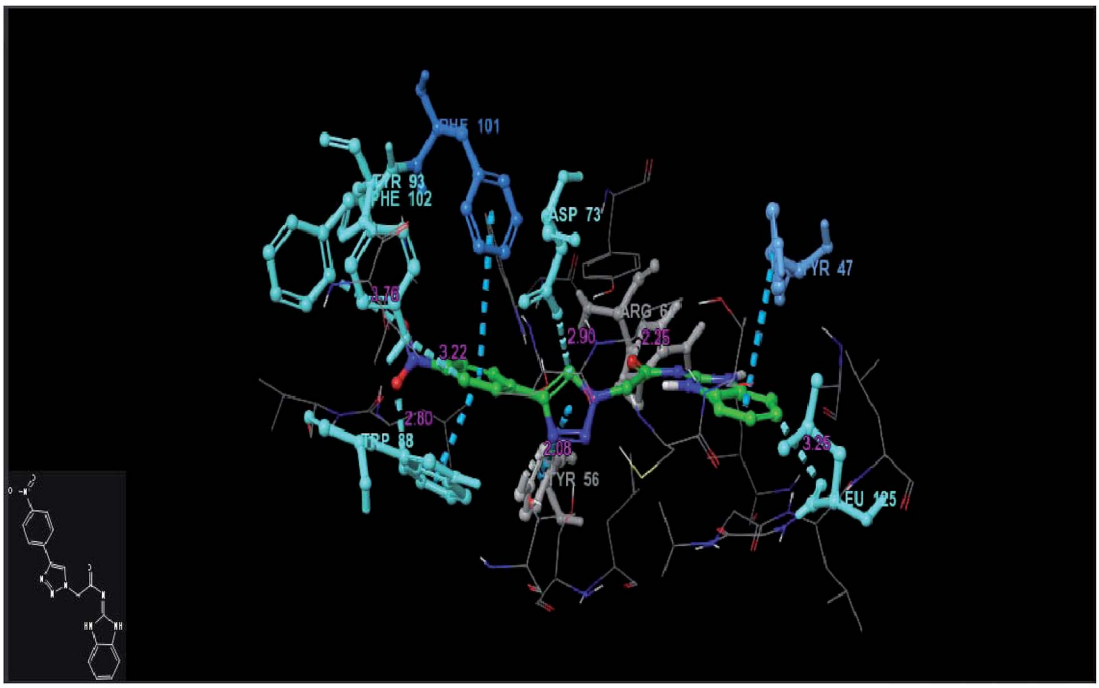

Fig. 7 Docked pose view of compound **6p** inside the 2UV0, showing interactions and distances (color interpretation: white-hydrogen bond, blue pi–pi stacking).

concentrations using BG45 as a positive control. Most of the compounds have low cytotoxicity at all tested concentrations using MTT assay (Fig. 4).[38]

In silico prediction of drug likeness properties

Physicochemical parameters of the designed compounds were *in silico* predicted using Qik-prop module of Schrödinger.[39,40] The *in silico* predicted values of physico-chemical parameters

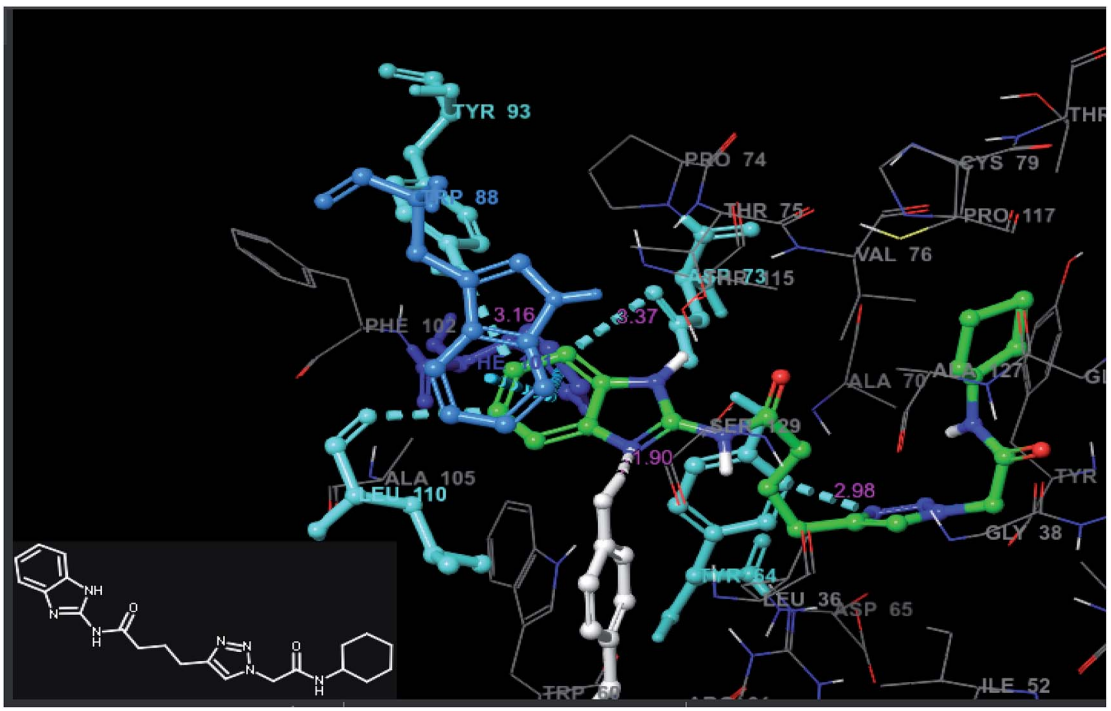

Fig. 8 Docked pose view of compound **11b** inside the 2UV0, showing interactions and distances (color interpretation: white-hydrogen bond, blue pi–pi stacking).

Table 4 Crystal data and structure refinement for **6d**

Identification code	**6d** (exp_399-AB-4R)
Empirical formula	$C_{20}H_{28}N_6O$
Formula weight	368.48
Temperature/K	293(2)
Crystal system	Monoclinic
Space group	$P2_1/c$
a/Å	18.8646(7)
b/Å	5.4019(2)
c/Å	20.0357(6)
α/°	90
β/°	90.614(3)
γ/°	90
Volume/Å^3	2041.61(12)
Z	4
ρ_{calc}g/cm^3	1.199
μ/mm^{-1}	0.619
F(000)	792.0
Crystal size/mm^3	0.5 × 0.02 × 0.01
Radiation	CuKα (λ = 1.54184)
2Θ range for data collection/°	8.828 to 159.794
Index ranges	$-23 \le h \le 23$, $-6 \le k \le 3$, $-23 \le l \le 25$
Reflections collected	10 329
Independent reflections	4308 [R_{int} = 0.0482, R_{sigma} = 0.0635]
Data/restraints/parameters	4308/0/245
Goodness-of-fit on F^2	1.063
Final R indexes [$I \ge 2\sigma$ (I)]	R_1 = 0.0671, wR_2 = 0.1867
Final R indexes [all data]	R_1 = 0.0834, wR_2 = 0.2036
Largest diff. peak/hole/e Å^{-3}	0.42/−0.27

for the titled compounds (**6a–q**, **7a–n**, **10a–b**, **11a–d**, **12a–c**) were shown in Table 3. Furthermore, ranges of these parameters followed by 95% of market approved drugs are given as footnotes of Table 3 (ref. 41 and 42) for comparison.

The predicted values of these parameters revealed that all the parameters like mol. wt., hydrogen bond donors (HBD), hydrogen bond acceptors (HBA), solvent accessible surface area (SASA), partition co-efficient (log P), predicted apparent Caco-2

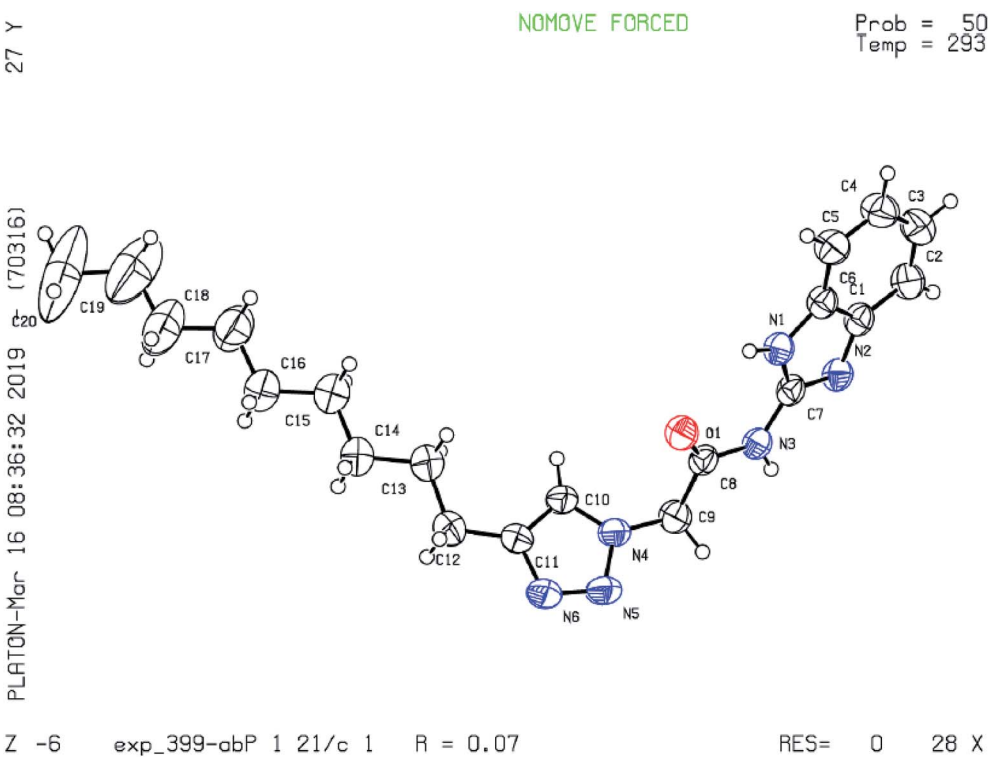

Fig. 9 ORTEP crystal structure diagram of compound.

cell permeability (PCaco), predicted brain/blood partition coefficient (log BB), aqueous solubility (log S) and number of rotatable bonds (Rot) were found within acceptable range and followed Lipinski rule of five. So overall, based upon the predicted values of these physico-chemical parameters, all the titled compounds possessed the drug-likeness behavior.

Docking studies

We performed molecular docking to investigate the binding mode of most active QSI **6p** with LasR receptor by the X-ray structure (PDB ID: 2UV0). For the docking study, we selected co-crystal structure as the source of the target taken is from the organism *P. aeruginosa* LasR and its resolution is better compared to other available PDB structures. Moreover, all the titled compounds were screened against the strain of *P. aeruginosa* and hence we took the same species for docking to get better correlation.

Docking studies of the significantly active compound (**6p**) and least active compound (**11b**) was performed using Glide 5.9 (ref. 43) running on maestro version 9.4, to investigate their putative binding mode with the target protein. Enzyme used for the docking study was LasR receptor protein (PDB: 2UV0) of *P. aeruginosa*, retrieved from RCSB, Protein Data Bank.[44] Protein preparation wizard of Schrödinger suite was used for preparation of target protein.

In order to predict the nature of binding mode of significant and least active compounds (**6p** and **11b** respectively) with the target protein, docking studies were carried out. The value of RMSD obtained between X-ray pose and re-docked pose (Fig. 5) for co-crystallized ligand in target protein was found to be 1.55 Å, suggesting that docking protocol could be relied on for the docking studies. The best docked pose (docking score −8.62) view of the co-crystallized ligand inside the active site of the target protein (PDB ID: 2UV0) is shown in Fig. 6. The figure revealed that, the co-crystallized ligand exhibited four hydrogen bond interactions with TYR 56 (2.29 Å), TRP 60 (2.12 Å), ASP 73 (1.94 Å) and SER 129 (2.22 Å) amino acid residues of the protein and two pi–pi stacking interactions (3.39 and 3.36 Å) respectively.

The analysis of best docked pose (Fig. 7) of compound **6p** (docking score −8.40) revealed that, the compound showed hydrogen bond interaction with TYR 56 (2.08 Å) and ASP 73 (2.90 Å) as that of co-crystallized ligand and also formed hydrogen bond interactions with ARG 61 (2.25 Å), TYR-93 (3.76 Å), LEU-125 (3.25 Å) and TRP-88 (2.80 Å) residues of the target. The compound also exhibited three pi–pi stacking interactions with TYR-47 (2.25 Å), TRP-88 (2.80 Å) and PHE-101 (3.22 Å) residues of the target protein and hence might stabilize its binding affinity with the target receptor, consequently may be responsible for its significant *in vitro* activity. The best docked pose (Fig. 8) of compound **11b** (docking score −9.06) displayed weak hydrogen bond interactions between TYR-64 (2.96 Å), TYR-93 (1.90 Å) and ASP 73 (3.37 Å) residues of target protein. The compound also exhibited pi–pi stacking interactions with Trp-88 (3.16 Å) residues. This weak binding affinity of compound **11b** may be responsible for its lower activity in the *in vitro* assay.

Single crystal X-ray crystallographic structure of compound 6d

The suitable crystals of the compound **6d** for X-ray crystallographic study were grown from the mixture of methanol and dichloromethane (1 : 1) solution. The single crystal X-ray diffraction measurement of the molecule ($C_{20}H_{28}N_6O$) was on Rigaku XtaLAB P200 diffract meter using graphite monochromated Cu-Ka radiation (λ = 1.54184 Å) on 0.5 mm × 0.02 mm × 0.01 mm colorless crystal. Data were collected and processed using CrysAlisPro (Rigaku Oxford Diffraction). The data were collected at a temperature of 293 K to a maximum $2q$ value of 159.794°. Of the 10 329 reflections were collected, where 4308 were unique (R_{int} = 0.0482) and equivalent reflections were merged. The crystal was kept at 293(2) K during data collection. Using Olex2, the structure was solved with the ShelX structure solution program using Direct Methods and refined with the ShelXL refinement package using least squares minimization. The basic crystallographic data are shown in Table 4. The molecular structure of the compound with methanol and dichloromethane solvents of crystallization is given as an ORTEP diagram in Fig. 9. The chain of nine carbons with C12 is directly bonded to C11 with more rigidity. As we move from C12 to C20, since the molecule is continuously undergoing vibration the terminal C20 with more flexibility experiences higher degree of vibrations as compare to C12. Therefore, the thermal parameters increase as we go from C12 to C20 and it is highest for C20. Crystallographic data for the compound **6d** have been deposited to the Cambridge Crystallographic Data Center and corresponding deposition number is CCDC 1904042.

3. Conclusion

In conclusion, series of novel 1,2,3-triazole derivatives of 2-aminobenzimidazole and 2-amino-5,6-dimethylbenzimidazole were designed and synthesized. All synthesized compounds were characterised using ^{1}H NMR, ^{13}C NMR, mass spectrometry and elemental analyses. The QSI activity of all 40 final compounds was evaluated against *P. aeruginosa* MH602. Among all derivatives, three compounds, **6i**, **6o**, **6p** and **7l** exhibited promising QSI activity of 64.99, 64.25, 68.23 and 65.80% against *P. aeruginosa* MH602 at 250 μM, respectively. These three compounds also exhibited significant activity at low concentrations (125 and 62.5 μM). Like, previously reported triazole based AHL analogues (**III** and **IV**), **6p** exhibited greatest QSI activity at low concentrations with 63.67% inhibition at 62.5 μM. These compounds were not found to be toxic when treated in normal cell line (HEK cell line) at 25, 50 and 100 μM. Hence, these compounds may become good starting point for further refinement in order to emerge as potent molecules with maximum therapeutic effect.

4. Experimental section

Materials and methods

All chemical reagents and solvents are purchased from Aldrich, Alfa Aesar, Finar. The solvents and reagents were of LR grade. All the solvents were dried and distilled before use. Thin-layer

chromatography (TLC) was carried out on aluminium-supported silica gel plates (Merck 60 F254) with visualization of components by UV light (254 nm). Column chromatography was carried out on silica gel (Merck 100–200 mesh). ^{1}H NMR and ^{13}C NMR spectra were recorded at 400 MHz and 101 MHz respectively using a Bruker AV 400 spectrometer (Bruker CO., Switzerland) in $CDCl_3$ and DMSO-d_6 solution with tetramethylsilane as the internal standard and chemical shift values (δ) were given in ppm. ^{1}H NMR spectra were recorded in $CDCl_3$ or DMSO-d_6. The following abbreviations are used to designate multiplicities: s = singlet, d = doublet, t = triplet, m = multiplet, br = broad. Melting points were determined on an electro thermal melting point apparatus (Stuart-SMP30) in open capillary tubes and are uncorrected. Elemental analyses were performed by Elementar Analysensysteme GmbH vario MICRO cube CHN Analyzer. Mass spectra (ESI-MS) were recorded on Schimadzu MS/ESI mass spectrometer.

General synthetic procedure for compounds 6a–q and 7a–n

A solution of azide (**5a**) (0.5 g, 2.3 mmol) in DMF : H_2O (8 : 2) was reacted with various substituted acetylenes (0.24 g, 3.5 mmol) in the presence of sodium ascorbate (0.023 g, 5 mol%), $CuSO_4 \cdot 5H_2O$ (0.006 g, 1 mol%). The reaction mixture was stirred at rt for 6–24 h. The reaction mixture was monitored by TLC. Upon completion of the reaction, as indicated by TLC, the reaction was diluted with ethyl acetate and washed with water. Organic layer was dried over anhydrous sodium sulphate, concentrated under reduced pressure and the crude residue was purified by column chromatography using 60–90% ethyl acetate in hexane as eluent to give 0.57 g of the title compound *N*-(1*H*-benzo[*d*]imidazol-2-yl)-2-(4-propyl-1*H*-1,2,3-triazol-1-yl)acetamide (**6a**) (yield: 88%). Similar procedure was followed to get the compounds **6b–q** and **7a–n** from **5a** and **5b** respectively.

General synthetic procedure for 9a–c

To a solution of compound (**2a**) (0.5 g, 3.776 mmol) in DMF (8.0 mL) at 0 °C was added EDC–HCl (1.08 g, 5.64 mmol), diisopropyl ethylamine (1.33 mL, 9.4 mmol), and HOBt (0.76 g, 5.664 mmol). The reaction mixture was stirred at rt for 16 h. Upon completion of the reaction, as indicated by TLC, DCM was added to the reaction mixture and washed with 10% bicarbonate and brine solution. The organic layer was dried over anhydrous Na_2SO_4 and concentrated *in vacuo*. The crude product was purified by column chromatography using 50–70% ethyl acetate in hexane as eluent to yield 0.66 g of *N*-(1*H*-benzo[*d*]imidazol-2-yl)pent-4-ynamide (**9a**). Similar procedure was followed for preparation of **9a–c** from **2a** and **2b**. Yield: **9a**: 82%; **9b**: 78% and **9c**: 80% (pale brown solids).

General synthetic procedure for 10a–c, 11a–d and 12a–c

A solution of alkyne (**9a**) (0.5 g, 2.3 mmol) in DMF : H_2O (8 : 2) was reacted with 2-azido-*N*-cyclohexylacetamide (**B**) (0.24 g, 2.34 mmol) in the presence of sodium ascorbate (0.023 g, 5 mol%), $CuSO_4 \cdot 5H_2O$ (0.006 g, 1 mol%). The reaction mixture was stirred at rt for 12 h. Upon completion of the reaction, as indicated by TLC, the reaction was diluted with ethyl acetate and washed with water. Organic layer was dried over anhydrous sodium sulphate, concentrated under reduced pressure and the crude residue was purified by column chromatography using 60–90% ethyl acetate in hexane as eluent to give 0.42 g of *N*-(1*H*-benzo[*d*]imidazol-2-yl)-3-(1-(2-(cyclohexylamino)-2-oxoethyl)-1*H*-1,2,3-triazol-4-yl)propanamide (**10a**; yield 46%). Similar procedure was followed in the synthesis of **10b**, **11a–d** and **12a–c** from **9a**, **9b** and **9c** respectively.

Analytical data for the final compounds

***N*-(1*H*-Benzo[*d*]imidazol-2-yl)-2-(4-propyl-1*H*-1,2,3-triazol-1-yl)acetamide (6a).** Pale green; (88%); m.p. 238–240 °C; IR ν_{max} (KBr, cm^{-1}) 3392, 3124, 2959, 1637, 1598; ^{1}H NMR (400 MHz, DMSO) δ 12.05 (s, 2H), 7.81 (s, 1H), 7.33 (dd, J = 5.9, 3.2 Hz, 2H), 6.98 (dd, J = 5.9, 3.2 Hz, 2H), 5.27 (s, 2H), 2.54 (t, 2H), 1.54 (sextet, 2H), 0.84 (t, 3H). ^{13}C NMR (101 MHz, DMSO) δ 168.17 147.83, 147.04, 135.44, 124.02, 121.95, 114.13, 52.77, 27.47, 22.77, 14.0. ESI-MS: (m/z) calcd for $C_{14}H_{16}N_6O$: 284.32, found 283.00 (M–H)$^+$; anal. calcd for $C_{14}H_{16}N_6O$: (%) C, 59.14; H, 5.67; N, 29.56; O, 5.63 found: C, 59.18; H, 5.63; N, 29.60; O, 5.59.

***N*-(1*H*-Benzo[*d*]imidazol-2-yl)-2-(4-pentyl-1*H*-1,2,3-triazol-1-yl)acetamide (6b).** Off white; (76%); m.p. 224–226 °C; IR ν_{max} (KBr, cm^{-1}) 3386, 3141, 2957, 1639, 1592, 1403; ^{1}H NMR (400 MHz, DMSO) δ 12.13 (s, 2H), 7.89 (s, 1H), 7.43 (dd, J = 5.9, 3.2 Hz, 2H), 7.12 (dd, J = 5.9, 3.2 Hz, 2H), 5.36 (s, 2H), 2.64 (t, 2H), 1.72–1.52 (m, 2H), 1.41–1.25 (m, 4H), 0.88 (t, 3H). ^{13}C NMR (101 MHz, DMSO) δ 168.15, 147.81 (s), 147.19, 135.31, 123.89, 121.96, 114.12, 52.77, 31.22, 29.20, 25.39, 22.33, 14.36. ESI-MS: (m/z) calcd for $C_{16}H_{20}N_6O$: 312.37, found 311.00 (M–H)$^+$; anal. calcd for $C_{16}H_{20}N_6O$: (%) C, 61.52; H, 6.45; N, 26.90; O, 5.12 found: C, 61.54; H, 6.43; N, 26.92; O, 5.10.

***N*-(1*H*-Benzo[*d*]imidazol-2-yl)-2-(4-heptyl-1*H*-1,2,3-triazol-1-yl)acetamide (6c).** White; (63%); m.p. 218–220 °C; IR ν_{max} (KBr, cm^{-1}) 3373, 3144, 2948, 1632, 1594, 1401; ^{1}H NMR (400 MHz, DMSO) δ 12.11 (s, 2H), 7.84 (s, 1H), 7.41 (dd, J = 5.9, 3.2 Hz, 2H), 7.032 (dd, J = 5.9, 3.2 Hz, 2H), 5.35 (s, 2H), 2.53 (t, 2H), 1.61–1.49 (m, 4H), 1.39–1.22 (m, 6H), 0.87 (t, 3H). ^{13}C NMR (101 MHz, DMSO) δ 168.03, 147.69, 147.24, 135.08, 123.45, 121.74, 114.11, 52.18, 31.34, 29.20, 28.12, 25.39, 24.46, 22.33, 14.36. ESI-MS: (m/z) calcd for $C_{18}H_{24}N_6O$: 340.42, found 339.00 (M–H)$^+$; anal. calcd for $C_{18}H_{24}N_6O$: (%) C, 63.51; H, 7.11; N, 24.69; O, 4.70 found: C, 63.54; H, 7.17; N, 24.66; O, 4.64.

***N*-(1*H*-Benzo[*d*]imidazol-2-yl)-2-(4-nonyl-1*H*-1,2,3-triazol-1-yl)acetamide (6d).** White; (55%); m.p. 215–217 °C; IR ν_{max} (KBr, cm^{-1}) 3339, 3142, 2962, 1634, 1591, 1402; ^{1}H NMR (400 MHz, DMSO) δ 12.13 (s, 2H), 7.89 (s, 1H), 7.45–7.40 (dd, J = 5.9, 3.2 Hz, 2H), 7.12 (dd, J = 5.9, 3.2 Hz, 2H), 5.35 (s, 2H), 2.66 (t, 2H), 1.59 (m, 2H), 1.36–1.23 (m, 12H), 0.86 (t, 3H). ^{13}C NMR (101 MHz, DMSO) δ 168.01, 147.62, 147.13, 134.19, 122.46, 121.21, 113.08, 52.47, 31.34, 29.81, 29.74, 29.11, 28.12, 25.39, 24.46, 22.33, 14.36. ESI-MS: (m/z) calcd for $C_{20}H_{28}N_6O$: 368.48, found 367.00 (M–H)$^+$; anal. calcd for

$C_{20}H_{28}N_6O$: (%) C, 65.19; H, 7.66; N, 22.81; O, 4.34 found: C, 65.20; H, 7.69; N, 22.80; O, 4.31.

***N*-(1*H*-Benzo[*d*]imidazol-2-yl)-2-(4-nonyl-1*H*-1,2,3-triazol-1-yl)acetamide (6e).** White; (92%); m.p. 201–203 °C; IR ν_{max} (KBr, cm^{-1}) 3391, 3136, 1641, 1583, 1399; ^1H NMR (400 MHz, DMSO) δ 12.62 (s, 1H), 12.14 (s, 2H), 8.13 (s, 1H), 7.52 (m, 1H), 7.41 (dd, J = 5.9, 3.1 Hz, 3H), 7.24–6.99 (m, 4H), 5.38 (s, 2H), 4.68 (s, 2H). ^{13}C NMR (101 MHz, DMSO) δ 168.27, 150.05, 147.99, 144.11, 143.56, 125.67, 122.03, 121.65, 117.94, 114.01, 110.87, 53.04, 28.28. ESI-MS: (m/z) calcd for $C_{19}H_{16}N_8OS$: 404.45, found 403.00 $(M–H)^+$; anal. calcd for $C_{19}H_{16}N_8OS$: (%) C, 56.42; H, 3.99; N, 27.71; O, 3.96; S, 7.93 found: C, 56.38; H, 4.12; N, 27.69; O, 3.97; S, 7.97.

***N*-(1*H*-Benzo[*d*]imidazol-2-yl)-2-(4-((5-chloro-2-oxopyridin-1(2*H*)-yl)methyl)-1*H*-1,2,3-triazol-1-yl)acetamide (6f).** White; (86%); m.p. 276–278 °C; IR ν_{max} (KBr, cm^{-1}) 3395, 3135, 1648, 1583, 1398; ^1H NMR (400 MHz, DMSO) δ 12.15 (s, 2H), 8.14 (s, 1H), 8.10 (dd, J = 7.5, 3.0 Hz, 1H), 7.50 (dt, J = 8.9, 4.4 Hz, 1H), 7.45–7.35 (m, 2H), 7.19–7.06 (m, 2H), 6.46 (t, J = 8.9 Hz, 1H), 5.40 (s, 2H), 5.16 (s, 2H). ^{13}C NMR (101 MHz, DMSO) δ 168.21, 160.26, 147.99, 142.43, 141.19, 137.22, 134.97, 126.12, 122.02, 121.37, 114.02, 110.86, 53.02, 44.02. ESI-MS: (m/z) calcd for $C_{17}H_{14}ClN_7O_2$: 383.79, found 382.00 $(M–H)^+$; anal. calcd for $C_{17}H_{14}ClN_7O_2$: (%) C, 53.20; H, 3.68; Cl, 9.24; N, 25.55; O, 8.34 found: C, 53.25; H, 3.65; Cl, 9.28; N, 25.53; O, 8.30.

***N*-(1*H*-Benzo[*d*]imidazol-2-yl)-2-(4-phenyl-1*H*-1,2,3-triazol-1-yl)acetamide (6g).** Brown; (45%); m.p. 272–274 °C; IR ν_{max} (KBr, cm^{-1}) 3385, 3101, 1646, 1595, 1401; ^1H NMR (400 MHz, DMSO) δ 12.15 (s, 2H), 8.62 (m, 2H), 8.13 (s, 1H), 7.79–7.40 (m, 4H), 7.31–6.83 (m, 3H), 5.46 (s, 2H). ^{13}C NMR (101 MHz, DMSO) δ 168.51, 147.23, 142.71, 141.38, 136.48, 135.82, 125.21, 124.98, 122.02, 121.37, 114.02, 54.01. ESI-MS: (m/z) calcd for $C_{17}H_{14}N_6O$: 318.33, found 317.00 $(M–H)^+$; anal. calcd for $C_{17}H_{14}N_6O$: (%) C, 64.14; H, 4.43; N, 26.40; O, 5.03 found: C, 64.19; H, 4.42; N, 26.37; O, 5.01.

***N*-(1*H*-Benzo[*d*]imidazol-2-yl)-2-(4-(4-fluorophenyl)-1*H*-1,2,3-triazol-1-yl)acetamide (6h).** White; (54%); m.p. 283–285 °C; IR ν_{max} (KBr, cm^{-1}) 3381, 3135, 1632, 1589, 1406. ^1H NMR (400 MHz, DMSO) δ 12.09 (s, 2H), 8.36 (s, 1H), 7.87 (d, J = 8.5 Hz, 2H), 7.64 (m, 2H), 7.43 (dd, J = 6.7, 3.3 Hz, 2H), 7.12 (dd, J = 6.7, 3.3 Hz, 2H), 5.45 (s, 2H). ^{13}C NMR (101 MHz, DMSO) δ 168.63, 157.42, 148.37, 145.71, 134.89, 131.87, 130.16, 128.56, 124.14, 122.10, 121.26, 113.91, 54.45. ESI-MS: (m/z) calcd for $C_{17}H_{13}FN_6O$: 336.32, found 335.00 $(M–1)^+$; anal. calcd for $C_{17}H_{13}FN_6O$: (%) C, 60.71; H, 3.90; F, 5.65; N, 24.99; O, 4.76 found: C, 60.74; H, 3.92; F, 5.66; N, 24.96; O, 4.73.

***N*-(1*H*-Benzo[*d*]imidazol-2-yl)-2-(4-(4-chlorophenyl)-1*H*-1,2,3-triazol-1-yl)acetamide (6i).** White; (52%); m.p. 269–271 °C; IR ν_{max} (KBr, cm^{-1}) 3348, 3137, 1644, 1597, 1403; ^1H NMR (400 MHz, DMSO) δ 12.08 (s, 2H), 8.37 (s, 1H), 7.72 (d, J = 8.5 Hz, 2H), 7.54 (d, J = 8.5 Hz, 2H), 7.41 (dd, J = 6.7, 3.3 Hz, 2H), 7.16–7.11 (m, 2H), 5.47 (s, 2H). ^{13}C NMR (101 MHz, DMSO) δ 168.65, 148.24, 146.52, 135.51, 132.45, 131.24, 130.86, 127.42, 123.87, 122.26, 121.27, 113.83, 53.41. ESI-MS: (m/z) calcd for $C_{17}H_{13}ClN_6O$: 397.23, found 395.00 $(M–2)^+$; anal. calcd for $C_{17}H_{13}ClN_6O$: (%) C, 51.40; H, 3.30; Br, 20.12; N, 21.16; O, 4.03 found: C, 51.43; H, 3.32; Br, 20.10; N, 21.15; O, 4.04.

***N*-(1*H*-Benzo[*d*]imidazol-2-yl)-2-(4-(4-bromophenyl)-1*H*-1,2,3-triazol-1-yl)acetamide (6j).** Brown; (82%); m.p. 292–294 °C; IR ν_{max} (KBr, cm^{-1}) 3354, 3112, 1629, 1594, 1403; ^1H NMR (400 MHz, DMSO) δ 12.20 (s, 2H), 8.38 (s, 1H), 7.85 (d, J = 8.5 Hz, 2H), 7.67 (d, J = 8.5 Hz, 2H), 7.42 (dd, J = 6.7, 3.3 Hz, 2H), 7.18–7.08 (m, 2H), 5.46 (s, 2H). ^{13}C NMR (101 MHz, DMSO) δ 168.63, 148.38, 145.63, 134.63, 132.40, 131.85, 130.52, 127.58, 123.86, 122.13, 121.28, 113.90, 53.41. ESI-MS: (m/z) calcd for $C_{17}H_{13}BrN_6O$: 397.23, found 395.00 $(M–2)^+$; anal. calcd for $C_{17}H_{13}BrN_6O$: (%) C, 51.40; H, 3.30; Br, 20.12; N, 21.16; O, 4.03 found: C, 51.43; H, 3.32; Br, 20.10; N, 21.15; O, 4.04.

***N*-(1*H*-Benzo[*d*]imidazol-2-yl)-2-(4-(*p*-tolyl)-1*H*-1,2,3-triazol-1-yl)acetamide (6k).** Off white; (70%); m.p. 281–283 °C; IR ν_{max} (KBr, cm^{-1}) 3376, 3132, 1645, 1597, 1405; ^1H NMR (400 MHz, DMSO) δ 12.19 (s, 2H), 8.56 (s, 1H), 7.77 (d, J = 8.0 Hz, 2H), 7.42 (dd, J = 6.6, 3.3 Hz, 2H), 7.28 (d, J = 8.0 Hz, 2H), 7.17–7.09 (m, 2H), 5.44 (s, 2H), 2.34 (s, 3H). ^{13}C NMR (101 MHz, DMSO) δ 168.51, 148.23, 146.73, 137.60, 129.73, 129.50, 128.50, 125.54, 123.06, 122.08, 113.95, 53.26, 21.30. ESI-MS: (m/z) calcd for $C_{18}H_{16}N_6O$: 332.36, found 331.00 $(M–H)^+$; anal. calcd for $C_{18}H_{16}N_6O$: (%) C, 65.05; H, 4.85; N, 25.29; O, 4.81 found: C, 65.11; H, 4.82; N, 25.30; O, 4.83.

***N*-(1*H*-Benzo[*d*]imidazol-2-yl)-2-(4-(4-(*tert*-butyl)phenyl)-1*H*-1,2,3-triazol-1-yl)acetamide (6l).** Off white; (67%); m.p. 265–267 °C; IR ν_{max} (KBr, cm^{-1}) 3362, 3123, 1642, 1599, 1404; ^1H NMR (400 MHz, DMSO) δ 12.07 (s, 2H), 8.51 (s, 1H), 7.76 (d, J = 8.0 Hz, 2H), 7.41 (dd, J = 6.6, 3.3 Hz, 2H), 7.18 (d, J = 8.0 Hz, 2H), 7.15–7.05 (m, 2H), 5.42 (s, 2H), 1.33 (s, 9H). ^{13}C NMR (101 MHz, DMSO) δ 168.43, 148.24, 146.71, 137.41, 129.01, 129.67, 128.61, 125.55, 123.09, 121.22, 114.05, 53.22, 35.79, 32.41. ESI-MS: (m/z) calcd for $C_{21}H_{22}N_6O$: 374.44, found 373.00 $(M–H)^+$; anal. calcd for $C_{21}H_{22}N_6O$: (%) C, 67.36; H, 5.92; N, 22.44; O, 4.27 found: C, 67.39; H, 5.90; N, 22.41; O, 4.29.

***N*-(1*H*-Benzo[*d*]imidazol-2-yl)-2-(4-(4-hydroxyphenyl)-1*H*-1,2,3-triazol-1-yl)acetamide (6m).** Brown gummy solid; (46%); IR ν_{max} (KBr, cm^{-1}) 3365, 3142, 1634, 1596, 1403; ^1H NMR (400 MHz, DMSO) δ 12.13 (s, 2H), 8.38 (s, 1H), 7.72 (d, J = 8.5 Hz, 2H), 7.41 (dd, J = 6.7, 3.3 Hz, 2H), 7.16–7.11 (m, 2H), 6.91 (d, J = 8.5 Hz, 2H), 6.7 (bs, 1H), 5.57 (s, 2H). ^{13}C NMR (101 MHz, DMSO) δ 168.43, 156.75, 148.23, 146.61, 135.42, 131.09, 130.81, 126.44, 123.88, 122.12, 121.23, 113.49, 54.98. ESI-MS: (m/z) calcd for $C_{17}H_{14}N_6O_2$: 334.33, found 333.00 $(M–2)^+$; anal. calcd for $C_{17}H_{14}N_6O_2$: (%) C, 61.07; H, 4.22; N, 25.14; O, 9.57 found: C, 61.10; H, 4.21; N, 25.15; O, 9.54.

***N*-(1*H*-Benzo[*d*]imidazol-2-yl)-2-(4-(4-methoxyphenyl)-1*H*-1,2,3-triazol-1-yl)acetamide (6n).** Pale yellow; (48%); m.p. 242–243 °C; IR ν_{max} (KBr, cm^{-1}) 3343, 3107, 1646, 1598, 1405; ^1H NMR (400 MHz, DMSO) δ 12.16 (s, 2H), 8.36 (s, 1H), 7.75 (d, J = 8.4 Hz, 2H), 7.62 (d, J = 8.4 Hz, 2H), 7.40 (dd, J = 6.7, 3.3 Hz, 2H), 7.16–7.07 (m, 2H), 5.46 (s, 2H), 3.78 (s, 3H). ^{13}C NMR (101 MHz, DMSO) δ 168.73, 159.41, 147.63, 135.13, 132.42, 131.87, 130.47, 127.64, 123.26, 122.14, 121.38, 113.91, 53.42, 54.47. ESI-MS: (m/z) calcd for $C_{18}H_{16}N_6O_2$: 348.36, found 347.00 $(M–2)^+$; anal. calcd for $C_{18}H_{16}N_6O_2$: (%) C,

62.06; H, 4.63; N, 24.12; O, 9.19 found: C, 62.11; H, 4.61; N, 24.11; O, 9.17.

***N*-(1*H*-Benzo[*d*]imidazol-2-yl)-2-(4-(4-(trifluoromethyl)phenyl)-1*H*-1,2,3-triazol-1-yl)acetamide (6o).** White; (72%); m.p. 286–288 °C; IR ν_{max} (KBr, cm^{-1}) 3383, 3107, 1654, 1599, 1404; ^{1}H NMR (400 MHz, DMSO) δ 12.06 (s, 2H), 8.66 (s, 1H), 7.96 (d, J = 8.1 Hz, 2H), 7.69 (d, J = 8.3 Hz, 2H), 7.31–7.24 (m, 2H), 7.02–6.95 (m, 2H), 5.33 (s, 2H). ^{13}C NMR (101 MHz, DMSO) δ 168.69, 148.44, 145.30, 135.23, 134.59, 128.62, 128.31, 126.44, 124.78, 123.38, 122.15, 113.87, 53.50. ESI-MS: (m/z) calcd for $C_{18}H_{13}F_3N_6O$: 386.33, found 385.00 $(M–H)^+$; anal. calcd for $C_{18}H_{13}F_3N_6O$: (%) C, 55.96; H, 3.39; F, 14.75; N, 21.75; O, 4.14 found: C, 60.01; H, 3.40; F, 14.72; N, 21.71; O, 4.15.

***N*-(1*H*-Benzo[*d*]imidazol-2-yl)-2-(4-(4-nitrophenyl)-1*H*-1,2,3-triazol-1-yl)acetamide (6p).** Pale yellow; (68%); m.p. 283–285 °C; IR ν_{max} (KBr, cm^{-1}) 3358, 3104, 1638, 1595, 1403; ^{1}H NMR (400 MHz, DMSO) δ 12.28 (s, 2H), 8.96 (s, 1H), 8.40 (d, J = 8.9 Hz, 2H), 8.23 (d, J = 8.8 Hz, 2H), 7.48 (dd, J = 5.9, 3.2 Hz, 2H), 7.25–7.12 (m, 2H), 5.56 (s, 2H). ^{13}C NMR (101 MHz, DMSO) δ 168.79, 148.54, 147.07, 147.78, 137.66, 126.37, 125.63, 124.93, 124.36, 122.19, 113.81, 53.62. ESI-MS: (m/z) calcd for $C_{17}H_{13}N_7O_3$: 363.33, found 362.00 $(M–H)^+$; anal. calcd for $C_{17}H_{13}N_7O_3$: (%) C, 56.20; H, 3.61; N, 26.99; O, 13.21 found: C, C, 56.24; H, 3.59; N, 26.96; O, 13.22.

***N*-(1*H*-Benzo[*d*]imidazol-2-yl)-2-(4-(3-nitrophenyl)-1*H*-1,2,3-triazol-1-yl)acetamide (6q).** Yellow; (64%); m.p. 240–242 °C; IR ν_{max} (KBr, cm^{-1}) 3357, 3120, 1642, 1596, 1403; ^{1}H NMR (400 MHz, DMSO) 12.26 (s, 2H), 8.91 (s, 1H), 8.32 (m, 2H), 8.21 (d, J = 6.8 Hz, 1H), 7.79 (t, J = 7.8 Hz, 1H), 7.42 (dd, J = 5.5, 3.1 Hz, 2H), 7.13 (dd, J = 5.4, 3.2 Hz, 2H), 5.49 (s, 2H). ^{13}C NMR (101 MHz, DMSO) δ 168.25, 148.44, 148.18, 147.13, 137.52, 1345.41, 133.46, 126.77, 125.47, 124.82, 124.53, 122.67, 113.22, 53.41. ESI-MS: (m/z) calcd for $C_{17}H_{13}N_7O_3$: 363.33, found 362.00 $(M–H)^+$; anal. calcd for $C_{17}H_{13}N_7O_3$: (%) C, 56.20; H, 3.61; N, 26.99; O, 13.21 found: C, 56.22; H, 3.57; N, 26.97; O, 13.21.

***N*-(5,6-Dimethyl-1*H*-benzo[*d*]imidazol-2-yl)-2-(4-propyl-1*H*-1,2,3-triazol-1-yl)acetamide (7a).** White; (73%); m.p. 241–243 °C; IR ν_{max} (KBr, cm^{-1}) 3367, 3134, 1692, 1598, 1401; ^{1}H NMR (400 MHz, DMSO) δ 11.99 (s, 2H), 7.88 (s, 1H), 7.18 (s, 2H), 5.30 (s, 2H), 2.62 (t, 2H), 2.26 (s, 6H), 1.69–1.56 (m, 2H), 0.93 (t, 3H). ^{13}C NMR (101 MHz, DMSO) δ 168.95, 148.07, 146.92, 132.79, 130.27, 123.90, 114.12, 53.13, 27.51, 22.79, 20.30, 14.05. ESI-MS: (m/z) calcd for $C_{16}H_{20}N_6O$: 312.37, found 300.00 $(M–H)^+$; anal. calcd for $C_{16}H_{20}N_6O$: (%) C, 61.52; H, 6.45; N, 26.90; O, 5.12 found: C, 61.56; H, 6.43; N, 26.86; O, 5.14.

***N*-(5,6-Dimethyl-1*H*-benzo[*d*]imidazol-2-yl)-2-(4-pentyl-1*H*-1,2,3-triazol-1-yl)acetamide (7b).** Off white; (66%); m.p. 200–202 °C; IR ν_{max} (KBr, cm^{-1}) 3374, 3132, 1682, 1584, 1407; ^{1}H NMR (400 MHz, DMSO) δ 12.09 (s, 2H), 7.87 (s, 1H), 7.18 (s, 2H), 5.29 (s, 2H), 2.64 (t, 2H), 2.26 (s, 6H), 1.64–1.56 (m, 2H), 1.32 (m, 4H), 0.87 (t, 3H). ^{13}C NMR (101 MHz, DMSO) δ 168.92, 147.98, 147.16, 132.91, 130.26, 123.85, 114.12, 53.14, 31.23, 29.19, 25.40, 22.33, 20.29, 14.35. ESI-MS: (m/z) calcd for $C_{18}H_{24}N_6O$: 340.42, found 339.00 $(M–H)^+$; anal. calcd for $C_{18}H_{24}N_6O$: (%) C, 63.51; H, 7.11; N, 24.69; O, 4.70 found: C, 63.54; H, 7.13; N, 24.67; O, 4.67.

***N*-(5,6-Dimethyl-1*H*-benzo[*d*]imidazol-2-yl)-2-(4-heptyl-1*H*-1,2,3-triazol-1-yl)acetamide (7c).** Grey colour; (57%); m.p. 209–211 °C; IR ν_{max} (KBr, cm^{-1}) 3369, 3124, 1691, 1594, 1403; ^{1}H NMR (400 MHz, DMSO) δ 12.12 (s, 2H), 7.87 (s, 1H), 7.18 (s, 2H), 5.29 (s, 2H), 2.36 (t, 2H), 2.26 (s, 2H), 1.62–1.50 (m, 6H), 1.38–1.23 (m, 8H), 0.84 (t, 3H). ^{13}C NMR (101 MHz, DMSO) δ 168.90, 147.96, 147.11, 132.91, 130.22, 123.81, 114.15, 53.16, 31.24, 29.13, 28.95, 25.41, 22.23, 20.29, 19.18, 14.36. ESI-MS: (m/z) calcd for $C_{20}H_{28}N_6O$: 368.48, found 367.00 $(M–H)^+$; anal. calcd for $C_{20}H_{28}N_6O$: (%) C, 65.19; H, 7.66; N, 22.81; O, 4.34 found: C, 65.23; H, 7.64; N, 22.77; O, 4.36.

***N*-(5,6-Dimethyl-1*H*-benzo[*d*]imidazol-2-yl)-2-(4-nonyl-1*H*-1,2,3-triazol-1-yl)acetamide (7d).** Off white; (55%); m.p. 194–196 °C; IR ν_{max} (KBr, cm^{-1}) 3358, 3112, 1684, 1598, 1406; ^{1}H NMR (400 MHz, DMSO) δ 12.03 (s, 2H), 7.87 (s, 1H), 7.18 (s, 2H), 5.29 (s, 2H), 2.63 (t, 2H), 2.25 (s, 6H), 1.60 (m, 2H), 1.31–1.28 (m, 4H), 1.27–1.23 (s, 8H), 0.85 (t, 3H). ^{13}C NMR (101 MHz, DMSO) δ 168.72, 148.47, 147.50, 133.55, 130.26, 123.66, 114.06, 53.13, 31.77, 29.54, 29.44, 29.29, 29.19, 29.05, 25.45, 22.57, 20.30, 14.42. ESI-MS: (m/z) calcd for $C_{22}H_{32}N_6O$: 396.53, found 395.00 $(M–H)^+$; anal. calcd for $C_{22}H_{32}N_6O$: (%) C, 66.64; H, 8.13; N, 21.19; O, 4.03 found: C, 66.66; H, 8.11; N, 21.17; O, 4.05.

2-(4-(((1*H*-Benzo[*d*]imidazol-2-yl)thio)methyl)-1*H*-1,2,3-triazol-1-yl)-*N*-(5,6-dimethyl-1*H*-benzo[*d*]imidazol-2-yl) acetamide (7e). Off white; (84%); m.p. 194–196 °C; IR ν_{max} (KBr, cm^{-1}) 3371, 3132, 1691, 1594, 1405; ^{1}H NMR (400 MHz, DMSO) δ 12.62 (s, 2H), 11.19 (s, 1H), 8.16 (s, 1H), 7.60 (m, 2H), 7.43 (dd, J = 5.9, 3.1 Hz, 2H), 7.19 (s, 2H), 5.37 (s, 2H), 4.43 (s, 2H), 2.31 (s, 6H). ^{13}C NMR (101 MHz, DMSO) δ 168.26, 150.24, 148.01, 144.08, 143.53, 125.67, 122.04, 121.68, 117.91, 114.00, 110.67, 53.06, 28.48, 20.18. ESI-MS: (m/z) calcd for $C_{21}H_{20}N_8OS$: 432.50, found 431.00 $(M–H)^+$; anal. calcd for $C_{21}H_{20}N_8OS$: (%) C, 58.32; H, 4.66; N, 25.91; O, 3.70; S, 7.41 found: C, 58.35; H, 4.68; N, 25.89; O, 3.69; S, 7.40.

2-(4-((5-Chloro-2-oxopyridin-1(2*H*)-yl)methyl)-1*H*-1,2,3-triazol-1-yl)-*N*-(5,6-dimethyl-1*H*-benzo[*d*]imidazol-2-yl) acetamide (7f). White; (83%); m.p. 281–283 °C; IR ν_{max} (KBr, cm^{-1}) 3369, 3131, 1694, 1593, 1409; ^{1}H NMR (400 MHz, DMSO) δ 12.01 (s, 2H), 8.11 (m, 2H), 7.51 (dd, J = 9.7, 2.9 Hz, 1H), 7.17 (s, 2H), 6.47 (d, J = 9.7 Hz, 1H), 5.33 (s, 2H), 5.17 (s, 2H), 2.26 (s, 6H). ^{13}C NMR (101 MHz, DMSO) δ 160.16, 142.36, 141.51, 141.51, 137.22, 136.84, 126.05, 121.37, 121.23, 113.99, 110.86, 53.41, 44.00, 20.29. ESI-MS: (m/z) calcd for $C_{19}H_{18}ClN_7O_2$: 411.84, found 410.00 $(M–H)^+$; anal. calcd for $C_{19}H_{18}ClN_7O_2$: (%) C, 55.41; H, 4.41; Cl, 8.61; N, 23.81; O, 7.77 found: C, 55.44; H, 4.43; Cl, 8.60; N, 23.80; O, 7.73.

***N*-(5,6-Dimethyl-1*H*-benzo[*d*]imidazol-2-yl)-2-(4-phenyl-1*H*-1,2,3-triazol-1-yl)acetamide (7g).** Dark brown gummy solid; (47%); IR ν_{max} (KBr, cm^{-1}) 3358, 3137, 1671, 1584, 1404; ^{1}H NMR (400 MHz, DMSO) δ 12.03 (s, 2H), 8.37 (s, 1H), 7.73 (d, J = 7.8 Hz, 2H), 7.41–7.32 (m, 3H), 7.17 (s, 2H), 5.34 (s, 2H), 2.23 (s, 6H). ^{13}C NMR (101 MHz, DMSO) δ 168.43, 147.18, 146.45, 136.89, 129.84, 1298.40, 127.51, 125.59, 122.34, 113.91, 53.25, 21.30. ESI-MS: (m/z) calcd for $C_{19}H_{18}N_6O$: 346.39, found 345.00 $(M–H)^+$; anal. calcd for $C_{19}H_{18}N_6O$: (%) C, 65.88; H, 5.24; N, 24.26; O, 4.62 found: C, 65.90; H, 5.28; N, 24.24; O, 4.58.

2-(4-(4-Bromophenyl)-1*H*-1,2,3-triazol-1-yl)-*N*-(5,6-dimethyl-1*H*-benzo[*d*]imidazol-2-yl)acetamide (7h). White; (76%); m.p. 273–275 °C; IR ν_{max} (KBr, cm^{-1}) 3349, 3137, 1691, 1588, 1407; ^{1}H

NMR (400 MHz, DMSO) δ 12.04 (s, 2H), 8.55 (s, 1H), 7.41 (dd, J = 6.7, 3.3 Hz, 2H), 7.12–7.09 (m, 2H), 7.18 (s, 2H), 5.37 (s, 2H), 2.26 (s, 6H). ^{13}C NMR (101 MHz, DMSO) δ 168.51, 148.17, 146.25, 137.11, 129.69, 129.41, 128.22, 125.69, 123.63, 122.34, 114.12, 53.24, 21.29. ESI-MS: (m/z) calcd for $C_{19}H_{17}BrN_6O$: 425.28, found 424.00 $(M–H)^+$; anal. calcd for $C_{19}H_{17}BrN_6O$: (%) C, 53.66; H, 4.03; Br, 18.79; N, 19.76; O, 3.76, found: C, 53.71; H, 4.00; Br, 18.77; N, 19.78; O, 3.74.

***N*-(5,6-Dimethyl-1*H*-benzo[*d*]imidazol-2-yl)-2-(4-(*p*-tolyl)-1*H*-1,2,3-triazol-1-yl)acetamide (7i).** Pale yellow; (55%); m.p. 258–260 °C; IR ν_{max} (KBr, cm^{-1}) 3386, 3127, 1639, 1592, 1404; ^{1}H NMR (400 MHz, DMSO) δ 12.06 (s, 2H), 8.54 (s, 1H), 7.76 (d, J = 7.8 Hz, 2H), 7.27 (d, J = 7.8 Hz, 2H), 7.18 (s, 2H), 5.37 (s, 2H), 2.34 (s, 3H), 2.26 (s, 6H). ^{13}C NMR (101 MHz, DMSO) δ 168.53, 148.17, 146.45, 137.89, 129.86, 129.40, 128.52, 125.59, 123.67, 122.33, 113.94, 53.25, 21.30, 20.24. ESI-MS: (m/z) calcd for $C_{20}H_{20}N_6O$: 360.41, found 359.00 $(M–H)^+$; anal. calcd for $C_{20}H_{20}N_6O$: (%) C, 66.65; H, 5.59; N, 23.32; O, 4.44 found: C, 66.68; H, 5.56; N, 23.34; O, 4.42.

***N*-(5,6-Dimethyl-1*H*-benzo[*d*]imidazol-2-yl)-2-(4-(4-hydroxyphenyl)-1*H*-1,2,3-triazol-1-yl)acetamide (7j).** Brown; (65%); m.p. 326–328 °C; IR ν_{max} (KBr, cm^{-1}) 3378, 3136, 1684, 1594, 1409; ^{1}H NMR (400 MHz, DMSO) δ 11.85 (s, 2H), 8.49 (s, 1H), 7.83 (d, J = 8.1 Hz, 2H), 7.66 (d, J = 8.2 Hz, 2H), 7.19 (s, 2H), 6.83 (bs, 1H) 5.22 (s, 2H), 2.23 (s, 6H). ^{13}C NMR (101 MHz, DMSO) δ 168.41, 148.34, 136.21, 131.69, 128.53, 128.24, 126.19, 126.37, 123.82, 122.39, 113.77, 53.58, 20.35. ESI-MS: (m/z) calcd for $C_{19}H_{18}N_6O_2$: 362.39, found 361.00 $(M–H)^+$; anal. calcd for $C_{19}H_{18}N_6O_2$: (%) C, 62.97; H, 5.01; N, 23.19; O, 8.83 found: C, 62.99; H, 5.04; N, 23.16; O, 8.81.

***N*-(5,6-Dimethyl-1*H*-benzo[*d*]imidazol-2-yl)-2-(4-(4-methoxyphenyl)-1*H*-1,2,3-triazol-1-yl)acetamide (7k).** Pale yellow; (58%); m.p. 283–285 °C; IR ν_{max} (KBr, cm^{-1}) 3338, 3127, 1672, 1598, 1402; ^{1}H NMR (400 MHz, DMSO) δ 12.03 (s, 2H), 8.49 (s, 1H), 7.96 (d, J = 8.1 Hz, 2H), 7.81 (d, J = 8.2 Hz, 2H), 7.00 (s, 2H), 5.36 (s, 2H), 3.78 (s, 3H) 2.23 (s, 6H). ^{13}C NMR (101 MHz, DMSO) δ 168.33, 148.42, 136.93, 131.17, 128.73, 126.81, 126.73, 123.64, 121.82, 113.37, 53.71, 51.47, 20.32. ESI-MS: (m/z) calcd for $C_{20}H_{20}N_6O_2$: 376.41, found 375.00 $(M–H)^+$; anal. calcd for $C_{20}H_{20}N_6O_2$: (%) C, 63.82; H, 5.36; N, 22.33; O, 8.50 found: C, 63.87; H, 5.34; N, 22.32; O, 8.49.

***N*-(5,6-Dimethyl-1*H*-benzo[*d*]imidazol-2-yl)-2-(4-(4-(trifluoromethyl)phenyl)-1*H*-1,2,3-triazol-1-yl)acetamide (7l).** Pale yellow; (66%); m.p. 273–275 °C; IR ν_{max} (KBr, cm^{-1}) 3385, 3142, 1694, 1527, 1402; ^{1}H NMR (400 MHz, DMSO) δ 11.93 (s, 2H), 8.64 (s, 1H), 7.96 (d, J = 8.1 Hz, 2H), 7.68 (d, J = 8.2 Hz, 2H), 7.03 (s, 2H), 5.22 (s, 2H), 2.10 (s, 6H). ^{13}C NMR (101 MHz, DMSO) δ 169.69, 145.24, 135.29, 130.54, 128.56, 128.24, 126.45, 126.09, 124.74, 123.39, 113.78, 53.91, 20.28. ESI-MS: (m/z) calcd for $C_{20}H_{17}F_3N_6O$: 314.38, found 313.00 $(M–H)^+$; anal. calcd for $C_{20}H_{17}F_3N_6O$: (%) C, 57.97; H, 4.14; F, 13.75; N, 20.28; O, 3.86 ffound: C, 57.99; H, 4.18; F, 13.74; N, 20.26; O, 3.83.

***N*-(5,6-Dimethyl-1*H*-benzo[*d*]imidazol-2-yl)-2-(4-(4-nitrophenyl)-1*H*-1,2,3-triazol-1-yl)acetamide (7m).** Pale yellow; (71%); m.p. 288–289 °C; IR ν_{max} (KBr, cm^{-1}) 3346, 3148, 1686, 1585, 1406; ^{1}H NMR (400 MHz, DMSO) δ 12.09 (s, 2H), 8.89 (s, 1H), 8.31 (d, J = 7.9 Hz, 2H), 8.16 (d, J = 7.9 Hz, 2H), 7.18 (s, 2H), 5.42 (s, 2H), 2.26 (s, 6H). ^{13}C NMR (101 MHz, DMSO) δ 169.68, 145.28, 135.45, 131.07, 128.67, 128.38, 127.02, 126.01, 124.75, 123.43, 113.76, 53.92, 20.29. ESI-MS: (m/z) calcd for $C_{19}H_{17}N_7O_3$: 391.38, found 390.00 $(M–H)^+$; anal. calcd for $C_{19}H_{17}N_7O_3$: (%) C, 58.31; H, 4.38; N, 25.05; O, 12.26 found: C, 58.33; H, 4.42; N, 25.01; O, 12.24.

***N*-(5,6-Dimethyl-1*H*-benzo[*d*]imidazol-2-yl)-2-(4-(3-nitrophenyl)-1*H*-1,2,3-triazol-1-yl)acetamide (7n).** Yellow; (67%); m.p. 277–279 °C; IR ν_{max} (KBr, cm^{-1}) 3328, 3137, 1649, 1598, 1389; ^{1}H NMR (400 MHz, DMSO) δ 12.08 (s, 2H), 8.89 (s, 1H), 8.73–8.63 (m, 1H), 8.33 (d, J = 7.9 Hz, 1H), 8.21 (d, J = 7.8, 1H), 7.78 (t, J = 8.0 Hz, 1H), 7.18 (s, 2H), 5.41 (s, 2H), 2.26 (s, 6H). ^{13}C NMR (101 MHz, DMSO) δ 169.67, 145.21, 135.34, 134.81, 131.18, 130.72, 128.69, 128.38, 127.13, 126.11, 124.74, 123.23, 113.77, 53.82, 20.27. ESI-MS: (m/z) calcd for $C_{19}H_{17}N_7O_3$: 391.38, found 390.00 $(M–H)^+$; anal. calcd for $C_{19}H_{17}N_7O_3$: (%) C, 58.31; H, 4.38; N, 25.05; O, 12.26 found: C, 58.32; H, 4.43; N, 25.02; O, 12.23.

***N*-(1*H*-Benzo[*d*]imidazol-2-yl)-3-(1-(2-(cyclohexylamino)-2-oxoethyl)-1*H*-1,2,3-triazol-4-yl)propanamide (10a).** White; (46%); m.p. 328–330 °C; IR ν_{max} (KBr, cm^{-1}) 3384, 3137, 1648, 1579, 1408; ^{1}H NMR (400 MHz, DMSO) 12.04 (s, 1H), 11.54 (s, 1H), 8.32 (d, 1H), 7.81 (s, 1H), 7.48 (dd, J = 5.9, 3.2 Hz, 2H), 7.05 (dd, J = 5.9, 3.2 Hz, 2H), 4.98 (s, 2H), 3.84 (p, 1H), 2.76 (t, 2H) 2.61 (t, 2H) 2.14–1.18 (m, 10H). ^{13}C NMR (101 MHz, DMSO) δ 172.75, 165.22, 146.48, 124.96, 124.49, 121.61, 121.67, 121.44, 51.96, 50.83, 32.64, 31.11, 25.06, 24.38, 23.86. ESI-MS: (m/z) calcd for $C_{20}H_{25}N_7O_2$: 395.46, found 394.00 $(M–H)^+$; anal. calcd for $C_{20}H_{25}N_7O_2$: (%) C, 60.74; H, 6.37; N, 24.79; O, 8.09 found: C, 60.78; H, 6.39; N, 24.77; O, 8.05.

***N*-(1*H*-Benzo[*d*]imidazol-2-yl)-3-(1-(2-oxo-2-(pyridin-2-ylamino)ethyl)-1*H*-1,2,3-triazol-4-yl)propanamide (10b).** White; (63%); m.p. 286–288 °C; IR ν_{max} (KBr, cm^{-1}) 3378, 3131, 1643, 1569, 1405; ^{1}H NMR (400 MHz, DMSO) δ 12.14 (s, 1H), 11.30 (s, 1H), 10.96 (s, 1H), 8.36 (s, 1H), 7.95–7.79 (m, 3H), 7.68–7.57 (m, 1H), 7.53–7.11 (m, 4H), 5.38 (s, 2H), 3.04–2.60 (m, 4H). ^{13}C NMR (101 MHz, DMSO) δ 171.92, 165.73, 151.89, 148.61, 145.99, 145.84, 139.15, 138.87, 124.38, 124.30, 121.69, 120.34, 113.96, 52.55, 31.13, 21.07. ESI-MS: (m/z) calcd for $C_{19}H_{18}N_8O_2$: 390.40, found 389.00 $(M–H)^+$; anal. calcd for $C_{19}H_{18}N_8O_2$: (%) C, 58.45; H, 4.65; N, 28.70; O, 8.20 found: C, 58.49; H, 4.62; N, 28.66; O, 8.23.

***N*-(1*H*-Benzo[*d*]imidazol-2-yl)-4-(1-(2-(cyclopentylamino)-2-oxoethyl)-1*H*-1,2,3-triazol-4-yl)butanamide (11a).** White; (62%); m.p. 261–263 °C; IR ν_{max} (KBr, cm^{-1}) 3372, 3131, 1660, 1577, 1420; ^{1}H NMR (400 MHz, DMSO) 12.07 (s, 1H), 11.50 (s, 1H), 8.30 (d, 1H), 7.84 (s, 1H), 7.47 (dd, J = 5.9, 3.2 Hz, 2H), 7.07 (dd, J = 5.9, 3.2 Hz, 2H), 4.99 (s, 2H), 4.00 (p, 1H), 2.81 (t, 2H) 2.79 (m, 1H), 2.08–1.29 (m, 11H). ^{13}C NMR (101 MHz, DMSO) 172.70, 165.23, 146.47, 124.16, 124.00, 121.61, 121.52, 121.39, 51.98, 51.02, 32.69, 31.14, 25.06, 24.91, 23.85. ESI-MS: (m/z) calcd for $C_{20}H_{25}N_7O_2$: 396.46, found 395.00 $(M–H)^+$; anal. calcd for $C_{20}H_{25}N_7O_2$: (%) C, 60.74; H, 6.37; N, 24.79; O, 8.09 found: C, 60.79; H, 6.34; N, 24.78; O, 8.08.

***N*-(1*H*-Benzo[*d*]imidazol-2-yl)-4-(1-(2-(cyclohexylamino)-2-oxoethyl)-1*H*-1,2,3-triazol-4-yl)butanamide (11b).** White;

(58%); m.p. 199–201 °C; IR ν_{max} (KBr, cm^{-1}) 3383, 3133, 1637, 1566, 1402; ^{1}H NMR (400 MHz, DMSO) 12.09 (s, 1H), 11.57 (s, 1H), 8.31 (d, 1H), 7.86 (s, 1H), 7.51 (dd, J = 5.9, 3.2 Hz, 2H), 7.14 (dd, J = 5.9, 3.2 Hz, 2H), 4.97 (s, 2H), 3.89 (p, 1H), 2.69 (t, 2H) 2.62 (t, 2H), 2.14–1.18 (m, 12H). ^{13}C NMR (101 MHz, DMSO) δ 172.71, 165.82, 146.73, 124.83, 124.47, 121.61, 121.66, 121.49, 51.95, 50.82, 32.66, 31.17, 27.53, 25.26, 24.40, 23.83. ESI-MS: (m/z) calcd for $C_{21}H_{27}N_7O_2$: 409.48, found 394.00 $(M-H)^+$; anal. calcd for $C_{21}H_{27}N_7O_2$: (%) C, 61.60; H, 6.65; N, 23.94; O, 7.81 found: C, 61.64; H, 6.61; N, 23.92; O, 7.83.

***N*-(1*H*-Benzo[*d*]imidazol-2-yl)-4-(1-(2-oxo-2-(pyridin-2-ylamino)ethyl)-1*H*-1,2,3-triazol-4-yl)butanamide (11c).** White; (68%); m.p. 258–259 °C; IR ν_{max} (KBr, cm^{-1}) 3394, 3125, 1652, 1563, 1404; ^{1}H NMR (400 MHz, DMSO) δ 12.24 (s, 1H), 11.54 (s, 1H), 10.97 (s, 1H), 8.37 (s, 1H), 7.97 (m, 2H), 7.74 (dd, J = 5.8, 3.5 Hz, 3H), 7.15 (m, 1H), 7.08 (m, 2H), 5.37 (s, 2H), 2.73 (t, 2H), 2.59 (t, 2H), 1.93 (p, 2H). ^{13}C NMR (101 MHz, DMSO) δ 176.80, 165.75, 151.90, 148.61, 146.79, 133.93, 124.47, 124.29, 121.65, 121.45, 120.37, 116.09, 113.98, 52.51, 33.55, 31.27, 24.93. ESI-MS: (m/z) calcd for $C_{20}H_{20}N_8O_2$: 304.43, found 403.00 $(M-H)^+$; anal. calcd for $C_{20}H_{20}N_8O_2$: (%) C, 59.40; H, 4.98; N, 27.71; O, 7.91 found: C, 59.43; H, 4.96; N, 27.68; O, 7.93.

***N*-(1*H*-Benzo[*d*]imidazol-2-yl)-4-(1-(4-nitrophenyl)-1*H*-1,2,3-triazol-4-yl)butanamide (11d).** Yellow; (59%); m.p. 263–265 °C; IR ν_{max} (KBr, cm^{-1}) 3396, 3143, 1654, 1566, 1405; ^{1}H NMR (400 MHz, DMSO) δ 12.08 (s, 1H), 11.61 (s, 1H), 8.93 (s, 1H), 8.51 (d, J = 8.9 Hz, 2H), 8.32 (d, J = 8.8 Hz, 2H), 7.43 (dd, J = 5.9, 3.2 Hz, 2H), 7.25–7.12 (m, 2H), 2.83 (*t*, 2H), 2.61 (t, 2H), 1.98 (p, 2H). ^{13}C NMR (101 MHz, DMSO) δ 168.72, 148.57, 147.37, 147.71, 137.26, 126.57, 125.63, 124.98, 124.31, 122.14, 113.88, 33.69, 31.73, 24.28. ESI-MS: (m/z) calcd for $C_{19}H_{17}N_7O_3$: 391.38, found 390.00 $(M-H)^+$; anal. calcd for $C_{19}H_{17}N_7O_3$: (%) C, 58.31; H, 4.38; N, 25.05; O, 12.26 found: C, 58.35; H, 4.41; N, 25.02; O, 12.22.

4-(1-(2-(Cyclopentylamino)-2-oxoethyl)-1*H*-1,2,3-triazol-4-yl)-*N*-(5,6-dimethyl-1*H*-benzo[*d*]imidazol-2-yl)butanamide (12a). White; (47%); m.p. 252–254 °C; IR ν_{max} (KBr, cm^{-1}) 3377, 3148, 1647, 1582, 1404; ^{1}H NMR (400 MHz, DMSO) δ 12.08 (s, 1H), 11.57 (s, 1H), 10.91 (s, 1H), 8.34 (s, 1H), 7.44 (s, 2H), 4.94 (s, 2H), 3.61 (m, 1H), 2.65 (t, 2H) 2.4–1.86 (m, 12H), 1.67–1.33 (m, 6H). ^{13}C NMR (101 MHz, DMSO) δ 172.74, 165.37, 146.38, 124.91, 124.80, 121.49, 121.24, 121.45, 51.96, 51.02, 35.64, 34.45, 32.57, 32.29, 25.05, 24.83. ESI-MS: (m/z) calcd for $C_{22}H_{29}N_7O_2$: 423.51, found 422.00 $(M-H)^+$; anal. calcd for $C_{22}H_{29}N_7O_2$: (%) C, 62.39; H, 6.90; N, 23.15; O, 7.56 found: C, 62.37; H, 6.88; N, 23.17; O, 7.58.

4-(1-(2-(Cyclohexylamino)-2-oxoethyl)-1*H*-1,2,3-triazol-4-yl)-*N*-(5,6-dimethyl-1*H*-benzo[*d*]imidazol-2-yl)butanamide (12b). White; (46%); m.p. 282–285 °C; IR ν_{max} (KBr, cm^{-1}) 3393, 3127, 1682, 1582, 1408; ^{1}H NMR (400 MHz, DMSO) δ 12.05 (s, 1H), 11.53 (s, 1H), 10.78 (s, 1H), 8.32 (s, 1H), 7.82 (s, 2H), 4.98 (s, 2H), 3.54 (m, 1H), 2.64 (t, 2H) 2.4–1.5 (m, 12H), 1.31–1.12 (m, 8H). ^{13}C NMR (101 MHz, DMSO) δ 172.69, 165.37, 146.42, 124.11, 124.08, 121.19, 121.22, 121.49, 51.98, 51.02, 35.37, 34.27, 32.69, 32.14, 25.06, 24.92, 23.86. ESI-MS: (m/z) calcd for $C_{23}H_{31}N_7O_2$: 437.54, found 436.00 $(M-H)^+$; anal. calcd for $C_{23}H_{31}N_7O_2$: (%) C, 63.14; H, 7.14; N, 22.41; O, 7.31 found: C, 63.17; H, 7.11; N, 22.43; O, 7.29.

***N*-(5,6-Dimethyl-1*H*-benzo[*d*]imidazol-2-yl)-4-(1-(2-oxo-2-(pyridin-2-ylamino)ethyl)-1*H*-1,2,3-triazol-4-yl)butanamide (12c).** White; (45%); m.p. 273–275 °C; IR ν_{max} (KBr, cm^{-1}) 3314, 3127, 1639, 1571, 1407; ^{1}H NMR (400 MHz, DMSO) δ 12.45 (s, 1H), 11.54 (s, 1H), 10.96 (s, 1H), 8.44 (s, 1H), 7.47 (s, 2H), 5.18 (s, 2H), 2.27 (t, 2H), 2.59 (s, 6H), 2.48 (t, 2H), 1.78 (p, 2H). ^{13}C NMR (101 MHz, DMSO) δ 174.84, 165.71, 150.91, 148.66, 146.19, 133.43, 124.46, 123.27, 121.45, 121.43, 120.37, 116.14, 113.88, 52.54, 33.54, 31.54, 24.97. ESI-MS: (m/z) calcd for $C_{22}H_{24}N_8O_2$: 432.48, found 431.00 $(M-H)^+$; anal. calcd for $C_{22}H_{24}N_8O_2$: (%) C, 61.10; H, 5.59; N, 25.91; O, 7.40 found: C, 61.14; H, 5.57; N, 25.87; O, 7.38.

Quorum sensing inhibition assay

Antibacterial activities of the synthesized compounds were evaluated by using *P. aeruginosa* MH602 lasB reporter strain (PlasB: gfp(ASV)) following the protocol developed by Hentzer *et al.*[37] The production of AHL signals by this reporter strain leads to an increase in product of unstable green fluorescent protein (GFP-ASV) as a function of an active QS system.

AHL dependent GFP expressing *P. aeruginosa* MH602 PlasB-gfp(ASV) harbouring a chromosomal fusion of the lasB promoter expressing Gfp(ASV) in response to 3-oxo-dodecanoyl HSL strains were cultured overnight in LB10. Strains were diluted (1 : 100) in ABT medium supplemented with 0.25% tryptone and 0.13% yeast extract and 200 μL of aliquots were dispensed to flat bottom 96-well plate wells (Sarstedt Australia). Cultures were supplemented with varying concentrations of synthetic compounds dissolved in DMSO. Control cultures were supplemented with equal amount of DMSO (1%). Plates were sealed with self-adhesive microplate sealers (TopSeal-A, PerkinElmer) to allow air diffusion and to prevent condensation. Cultures were incubated in a plate reader (EnSight Multimode Plate Reader, PerkinElmer) at 37 °C with shaking briefly prior to each reading and fluorescence (excitation, 485 nm; emission, 535 nm) and OD600 of cultures were measured every 30 min over 20 h. Ampicillin (100 μg mL^{-1}) and gentamicin (20 μg mL^{-1}) were supplemented to *P. aeruginosa* MH602 cultures.

Cytotoxicity assay

MTT assay. Cytotoxicity of the novel promising compounds was determined using MTT assay. 45 7.5×10^3 cells were seeded in 96 well plates and incubated overnight. Cells were treated with synthesized compounds at three concentrations (50 μM, 25 μM and 10 μM) in duplicates and incubated for 24 h. 50 μL of 5 mg mL^{-1} 3-(4,5-dimethylthiazol-2-yl)-2,5-diphenyltetrazolium bromide (MTT; Himedia Laboratories Pvt. Ltd., Mumbai, India) was added and incubated for 4 h. Formazan crystals were dissolved using DMSO and absorbance was measured using Spectramax M4 (Molecular Devices, USA).

Cell culture and assay procedure

All the compounds tested for their cytotoxicity against Human Embryonic Kidney (HEK) cell lines (procured from National Centre for Cell Science, Pune, India) were cultured in DMEM (high glucose media: AL007S, Dulbecco's modified eagle medium) with 10% fetal bovine serum (FBS) and 1% antibiotic (Pen strep: A001) incubated at 37 °C and 5% CO_2 atmosphere. All reagents were purchased from Himedia Laboratories Pvt. Ltd., Mumbai, India. Cells were seeded in a 96-well plate (Eppendorf 0030730119) with 100 μL of cell suspension containing 10^4 cells per well and incubated overnight. The DMSO solutions of the synthesized compounds and BG45 were prepared and they were further diluted to their respective concentrations of 25 μM, 50 μM, and 100 μM with the DMEM complete media. The cells were then treated with 100 μL of the compound solutions made in media along with a blank control containing DMSO in medium and BG45 as positive control and were incubated for 24 h. The culture medium was aspirated and subsequently, 50 μL of 5 mg mL^{-1} concentrated solution of MTT (3-(4,5-dimethylthiazol-2-yl)-2,5-diphenyltetrazolium bromide) in phenol red free DMEM was prepared and added in each well and further incubated for 3 h for the formation of formazan crystals. Later, 100 μL DMSO was added to the culture after aspirating media in the wells to dissolve the formazan crystals and the absorbance was measured using multi-well plate reader Spectramax (Molecular Devices, USA) at two different wavelengths of 570 nm and 650 nm. The % cell viability was calculated as a fraction of absorbance obtained from the treated cells from the absorbance of untreated control cells.[37]

Conflicts of interest

There are no conflicts of interest to declare.

Acknowledgements

KVGCS and SM thank DBT, New Delhi [BT/IN/Spain/39/SMl2017-18] for providing financial support. The financial assistance provided by DIST FIST grant (SR/FST/CSI-240/2012), New Delhi is gratefully acknowledged. SS thanks CSIR for providing SRF fellowship. Central analytical lab facilities of BITS Pilani Hyderabad campus are gratefully acknowledged. We are also thankful to UNSW School of Biotechnology and Biomolecular Sciences and UNSW School of Medical Sciences for their support.

References

1 M. Boyer and F. Wisniewski-Dyé, *FEMS Microbiol. Ecol.*, 2009, **1**, 1–19.
2 G. D. Geske, J. C. O'Neill, D. M. Miller, M. E. Mattmann and H. E. Blackwell, *J. Am. Chem. Soc.*, 2007, **129**, 13613–13625.
3 D. McDougald, W. H. Lin, S. A. Rice and S. Kjelleberg, *Biofouling*, 2006, **22**, 133–144.
4 M. E. Mattmann and H. E. Blackwell, *J. Org. Chem.*, 2010, **75**, 6737–6746.
5 A. Eberhard, A. L. Burlingame, C. Eberhard, G. L. Kenyon, K. H. Nealson and N. J. Oppenheimer, *Biochemistry*, 1981, **20**, 2444–2449.
6 D. A. Higgins, M. E. Pomianek, C. M. Kraml, R. K. Taylor, M. F. Semmelhack and B. L. Bassler, *Nature*, 2007, **45**, 883–886.
7 M. M. Marketon, M. R. Gronquist, A. Eberhard and J. E. González, *J. Bacteriol.*, 2002, **184**, 5686–5695.
8 https://www.cdc.gov/hai/organisms/gram-negative-bacteria.html.
9 H. A. Khan, F. K. Baig and R. Mehboob, *Asian Pac. J. Trop. Med.*, 2017, **7**, 478–482.
10 N. A. Bhawsar and M. Singh, *Int. J. Adv. Res.*, 2014, **6**, 778–783.
11 R. Manfredi, A. Nanetti, M. Ferri and F. Chiodo, *Eur. J. Clin. Microbiol. Infect. Dis.*, 2000, **19**, 248–253.
12 A. R. Hauser and J. Rello, *Severe Infections Caused by Pseudomonas Aeruginosa*, 2003, http://www.springer.com/gp/book/9781402074219(book).
13 C. Van Delden and B. H. Iglewski, *Emerging Infect. Dis.*, 1998, **4**, 551–560.
14 http://www.who.int/medicines/publications/WHO-PPL-Short_Summary_25FebET_NM_WHO.pdf.
15 http://www.who.int/news-room/fact-sheets/detail/antibiotic-resistance.
16 L. Fulghesu, C. Giallorenzo and D. Savoia, *J. Chemother.*, 2007, **19**, 388–391.
17 R. Kerstin, S. Anke and H. Volkhard, *Perspect. Med. Chem.*, 2016, **8**, 1–15.
18 N. Ni, M. Li, J. Wang and B. Wa, *Med. Res. Rev.*, 2009, **29**, 65–124.
19 C. Y. Chang, T. Krishnan, H. Wang, Y. Chen, W. F. Yin, Y. M. Chong, L. Y. Tan, T. M. Chong and K. G. Chan, *Sci. Rep.*, 2014, **4**, 1–8.
20 Y. Peng, J. Bi, J. Shi, Y. Li, X. Ye, X. Chen and Z. Yao, *Am. J. Infect. Control*, 2014, **42**, 1308–1311.
21 L. C. Antunes, R. B. Ferreira, M. M. Buckner and B. B. Finlay, *Microbiology*, 2010, **156**, 2271–2282.
22 P. Williams and M. Cámara, *Curr. Opin. Microbiol.*, 2009, **12**, 182–191.
23 https://www.springer.com/in/book/9788132219811.
24 S. Srinivasarao, S. Nizalapur, T. T. Yu, D. S. Wenholz, P. Trivedi, B. Ghosh, K. Rangan, N. Kumar and K. V. G. Chandra Sekhar, *ChemistrySelect*, 2018, **3**, 9170–9180.
25 J. Musk, J. Dinty and P. J. Hergenrother, *Curr. Med. Chem.*, 2006, **13**, 2163–2177.
26 H. O. Sintim, J. A. Smith, J. Wang, S. Nakayama and L. Yan, *Future Med. Chem.*, 2010, **2**, 1005–1035.
27 J. J. Richards and C. Melander, *Anti-Infect. Agents Med. Chem.*, 2009, **4**, 295–314.
28 R. Frei, A. S. Breitbach and H. E. Blackwell, *Angew. Chem., Int. Ed.*, 2012, **51**, 5226–5229.
29 J. D Moore, J. P. Gerdt, N. R. Eibergen and H. E. Blackwell, *ChemBioChem*, 2014, **3**, 435–442.

30 D. Dheer, V. Singh and R. Shankar, *Bioorg. Chem.*, 2017, **71**, 30–54.
31 D. M. Stacy, S. T. Le Quement, C. L. Hansen, J. W. Clausen, T. T. Nielsen, J. W. Brummond, M. Givskov, T. E. Nielsen and H. E. Blackwella, *Org. Biomol. Chem.*, 2013, **11**, 938–954.
32 M. R. Hansen, T. H. Jakobsen, C. G. Bang, A. E. Cohrt, C. L. Hansen, J. W. Clausen, S. T. Le Quement, T. T. Nielsen, M. Givskov and T. E. Nielsen, *Bioorg. Med. Chem.*, 2015, **23**, 1638–1650.
33 G. Brackman, M. Risseeuw, S. Celen, P. Cos, L. Maes, H. J. Nelis, S. V. Calenbergh and T. Coenye, *Bioorg. Med. Chem.*, 2012, **20**, 4737–4743.
34 H. Nagesh, S. Singireddi, A. Suresh, S. Nizalapur, S. Murugesan, K. Kanneboina, N. Kumar and K. V. G. Chandra Sekhar, *ChemistrySelect*, 2018, **3**, 7565–7571.
35 S. Nizalapur, O. Kimyon, E. Yee, M. M. Bhadbhade, M. Manefield, M. Willcox, D. S. Black and N. Kumar, *Org. Biomol. Chem.*, 2017, **15**, 5743–5755.
36 https://patents.google.com/patent/WO2012174312A3/en.
37 M. Hentzer, K. Riedel, T. B. Rasmussen, A. Heydorn, J. B. Andersen, M. R. Parsek, S. A. Rice, L. Eberl, S. Molin and N. Høiby, *Microbiology*, 2002, **148**, 87–102.
38 J. Van Meerloo, G. J. Kaspers and J. Cloos, *Methods Mol. Biol.*, 2011, **731**, 237–245.
39 *Qikprop*, Schrödinger, LLC, New York, version 3.8, 2013.
40 S. Chander, A. Penta and S. Murugesan, *J. Pha. Res.*, 2014, **8**, 552–562.
41 *Qikprop, User Manual*, Schrödinger, LLC, version 4, 2014, ch. 1, pp. 2–5.
42 W. L. Jorgensen and E. M. Duffy, Prediction of drug solubility from Monte Carlo simulations, *Bioorg. Med. Chem. Lett.*, 2000, **10**, 1155–1158.
43 *Glide, Schrödinger, LLC*, New York, version 5.9, 2013.
44 L. K. Williams, C. Li, S. G. Withers and G. D. Brayer, *J. Med. Chem.*, 2012, **55**, 10177–10186.